The Etiology of Thumb Carpometacarpal Osteoarthritis: Early Indications from *In Vivo* Joint Contact Mechanics

By

Qi Zheng

Submitted to the graduate degree program in Bioengineering and the Graduate Faculty of the University of Kansas in partial fulfillment of the requirements for the degree of Master of Science in Bioengineering.

_____

Chairperson: Dr. Kenneth J. Fischer

_____

Dr. Paulette Spencer

_____

Dr. Sara Wilson

Date Defended:

The Dissertation Committee for Qi Zheng

certifies that this is the approved version of the following dissertation:

The Etiology of Thumb Carpometacarpal Osteoarthritis: Early Indications from *In Vivo* Joint Contact Mechanics

_____

Chairperson: Dr. Kenneth J. Fischer

Date approved:

## Abstract

The thumb carpometacarpal (CMC) joint is frequently affected by osteoarthritis (OA). The prevalence of thumb CMC OA greatly increases with age and has disproportional predominance in postmenopausal women. However, so far the etiology of thumb CMC OA remains unclear, and no conclusion has been achieved regarding the selection of the optimal surgical procedure. Joint contact mechanics can be an important aspect in understanding the mechanism of thumb CMC OA development. The contact pressure distribution on the articular surface directly affects the cartilage condition. This study quantitatively compared the *in vivo* thumb CMC joint contact mechanics between 4 males and 4 females using finite element modeling (FEM), and also evaluated the accuracy of a time-efficient surface-based contact modeling (SCM) procedure for possible clinical application. Although a sufficient statistical power cannot be achieved with the small number of subjects, the contact patterns were substantially different between male and female groups. Contact area, force and peak contact pressure showed a trend of increase in the older female subjects. Compared with FEM, the contact parameter values from SCM may be somewhat less accurate, but SCM produced contact distribution patterns similar to FEM. In addition, SCM was able to distinguish the different contact patterns between normal and osteoarthritic thumb CMC joints with much less data processing. Therefore, SCM has clear potential for future clinical diagnosis and the evaluation of treatment efficacy for thumb CMC OA.

This page left intentionally blank.

## Acknowledgements

**Proverbs 3:5-6 (NKJV)**

**5** Trust in the Lord with all your heart, and lean not on your own understanding;

**6** In all your ways acknowledge Him, and He shall direct your paths.

I would like to give my first and foremost gratitude to the salvation of the almighty God Who has been blessing me with His glorious riches and mercy through the cross of Jesus Christ. I would like to sincerely thank my advisor Dr. Ken Fischer, who has kindly given me the opportunity to work as a graduate research assistant in the Musculoskeletal Biomechanics Lab, and provided me extensive resources to complete my Master's program. I am very thankful for his extensive training and guidance that has allowed me to gained such precious knowledge and skills. I would like to thank my committee members Dr. Paulette Spencer and Dr. Sara Wilson for their tremendous input and genuine support throughout the duration of my graduate study and research. I would also like to give my thanks to Dr. Marylee Southard and Dr. Michael Detamore, for their mentoring when I was working as their graduate teaching assistant. I would like to extend my thankfulness to the faculty and staff of the Bioengineering Graduate Program, as well as my colleagues, for all the teaching and assistance I have received. It has been such a blessing to study and work with these excellent people. Meanwhile I would like to thank the Hoglund Brain Image Center for providing the access to their facility, which is an essential component for my thesis project. I would like to specially thank our post-doctoral fellow Dr. Joshua Johnson for his remarkable mentoring both in the lab and in many other aspects of my life. Last but not the least, I would like to deeply thank my family and friends for their unconditional love and support which have always been with me, even when we are thousands of miles apart.

This page left intentionally blank.

## Table of Content

Abstract ..... iii

Acknowledgements ..... v

Table of Content ..... vii

Nomenclature ..... 11

Table of Figures ..... 13

Motivation ..... 17

1 Background ..... 19

1.1 Anatomy ..... 19

1.2 Bones of the Thumb Basal Joint ..... 20

1.3 Muscles and Ligaments ..... 21

1.4 Thumb CMC Joint Osteoarthritis ..... 23

1.4.1 Prevalence, Incidence and Impact ..... 24

1.4.2 Staging, Diagnosis and Treatment ..... 25

1.4.3 Etiology ..... 27

1.4.4 Gender Differences ..... 28

1.5 Thumb Carpometacarpal Joint Contact Mechanics ..... 29

1.5.1 Prior Studies ..... 29

1.6 Modeling Procedures ..... 30

1.6.1 Finite Element Modeling ..... 31

1.6.2 Surface-Based Contact Modeling ..... 34

1.7 Conclusion and Motivations ..... 37

1.8 Reference ..... 38

2 Gender Differences and Aging Effects of *In Vivo* Thumb Carpometacarpal Joint Contact Mechanics ..... 47

2.1 Abstract ..... 51

2.2 Introduction ..... 51

2.3 Methods ..... 52

2.3.1 Subjects and MRI Scan ..... 52

2.3.2 Modeling Geometry ..... 53

2.3.3 Kinematic Transformation ..... 53

2.3.4 Modeling and Verification ..... 54

2.3.5 Statistical Analysis ..... 54

2.4 Results ..... 55

2.5 Discussion ..... 56

2.6 Conclusion ..... 60

2.7 Acknowledgments ..... 60

2.8 Funding ..... 60

2.9 References ..... 61

2.10 Tables and Figures ..... 64

3 *In Vivo* Thumb Carpometacarpal Joint Contact Mechanics: Comparison of Finite Element Modeling and Surface-based Contact Modeling ..... 75

3.1 Abstract ..... 79

3.2 Introduction ..... 79

3.3 Methods ..... 81

3.3.1 Subjects and MRI Scan ..... 81

3.3.2 Model Geometry Construction ..... 82

3.3.3 Kinematics ..... 83

3.3.4 Modeling Analyses and Verification ..... 83

3.4 Results ..... 85

3.5 Discussion ..... 86

3.6 Conclusion ..... 90

3.7 Acknowledgements ..... 90

3.8 Reference ..... 91

3.9 Tables and Figures ..... 93

4 Conclusion and Future Directions ..... 103

This page left intentionally blank.

## Nomenclature

2-D: two dimensional

3-D: three dimensional

3T: three Tesla

AOL: anterior oblique ligament

AP: average pressure

APL: abductor pollicis longus

BMI: body mass index

CA: contact area

CF: contact force

CMC: carpometacarpal

dAOL: deep anterior oblique ligament

DESS: dual echo steady state

DRL: dorsal radial ligament

ECRL: extensor carpi radialis longus

FCR: flexor carpi radialis

FEM: finite element modeling

MCP: metacarpophalangeal

MR/MRI: magnetic resonance imaging

IML: intermetacarpal ligament

OA: osteoarthritis

POL: posterior oblique ligament

PP: peak pressure

SAOL: superficial anterior oblique ligament

SCM: surface-based contact modeling

SCMU: surface-based contact modeling with uniform cartilage thickness

SCMV: surface-based contact modeling with variable cartilage thickness

TCL: transverse carpal ligament

UCL: ulnar collateral ligament

## Table of Figures

Figure 1.1. Left: location of the thumb CMC joint; right: saddle-shaped articular surfaces and perpendicular primary axes. Reprinted from The Journal of Biomechanics, Volume 25, Ateshian, G.A., Rosenwasser, M.P., and Mow, V.C., Curvature characteristics and congruence of the thumb carpometacarpal joint: differences between female and male joints, Pages 591-607, Copyright (1992), with permission from Elsevier. ..... 20

Figure 1.2. The bones articulating with trapezium include first and second metacarpal (MC I and MC II), trapezoid and scaphoid. Reprinted from http://commons.wikimedia.org/wiki/File:Carpus.jpg with modifications. ..... 21

Figure 1.3. Illustration of the major ligaments and some muscles in thumb CMC joint. Left: volar view, deep anterior oblique ligament (dAOL, brown), superficial anterior oblique ligament (SAOL, dark blue), volar first metacarpal ulnar base–second metacarpal radial base intermetacarpal ligament (v 1MC-2MC IML, yellow), ulnar collateral ligament (UCL, purple), transverse carpal ligament (TCL, red), flexor carpi radialis (FCR, light blue). Right: dorsal view, dorsal radial ligament (DRL, orange), posterior oblique ligament (POL, green), abductor pollicis longus (APL, brown), dorsal first metacarpal ulnar base–second metacarpal radial base intermetacarpal ligament (d 1MC-2MC IML, red), extensor carpi radialis longus (ECRL, yellow). Reprinted from The Journal of Hand Surgery, Volume 31, Nanno M., Buford W.L. Jr., Patterson R.M., Andersen C.R., Viegas S.F., Three-dimensional analysis of the ligamentous attachments of the first carpometacarpal joint, Pages 1160–1170, Copyright (2006), with permission from Elsevier. ..... 22

Figure 1.4. From left to right, Eaton Stage 1 - 4 thumb CMC OA as seen on a radiograph. Reprinted from The Journal of Hand Surgery, Volume 23, Barron, O.A., Eaton, R.G., Save the trapezium: Double interposition arthroplasty for the treatment of stage IV disease of the basal joint, Pages 196-204, Copyright (1998), with permission from Elsevier. ..... 25

Figure 1.5. Trapezium (bottom) and metacarpal (top) tetrahedral cartilage meshes for FEM. .... 32

Figure 1.6. Triangular bone surfaces (yellow) and bilinear cartilage surfaces (white) for trapezium and metacarpal for SCM ..... 36

Figure 2.1. (A) The unloaded MRI image of the trapezium and metacarpal. (B) The hand position and coil for the unloaded scan. ..... 65

Figure 2.2. (A) The loaded MRI image of the trapezium and metacarpal. (B) The hand position and coil for the loaded scan. (C) The visual feedback for the loaded scan..... 65

Figure 2.3. (A) Cartilage segmentation from the unloaded image. (B) 3-D cartilage volume generated in ScanIP..... 66

Figure 2.4. Unloaded image without mask (A), the segmented (B) and isolated (C) metacarpal bone without cartilage..... 66

Figure 2.5. Top: registration of loaded metacarpal (green) onto unloaded metacarpal (red). Bottom: registration of unloaded trapezium (green) onto transformed-loaded trapezium (red). Initial position is left (A), and aligned position is right (B)..... 67

Figure 2.6. Final finite element meshes of the trapezium cartilage (bottom) and metacarpal cartilage (top) articulation in the unloaded configuration in Abaqus. RP-2: reference point for the rigid body constraint. ..... 68

Figure 2.7. Example segmentation of direct contact area determined from a loaded image. ..... 68

Figure 2.8. MRI image of Subject F4 with osteophyte marked by the red circle. ..... 69
Figure 2.9. Mean value and standard deviation of contact measures for male and female groups. ..... 70
Figure 2.10. Regression of contact force onto age (top), peak pressure onto age (middle), and peak pressure on to body mass index (bottom) for males and females. ..... 71
Figure 2.11. Contact distribution on the trapezium and metacarpal for all subjects. Row 1: male trapezium; Row 2: male metacarpal; Row 3: female trapezium; Row 4: female metacarpal..... 72
Figure 2.12. Regression analysis of direct contact area and model contact area for all subjects, indicating a highly linear, significant relationship. ..... 73
Figure 3.1. Top: Unloaded scan, hand position (left) and MRI image (right). Bottom: Loaded scan, hand position (left) and MRI image (right). ..... 94
Figure 3.2. Top: Bone with cartilage segmentation (left) and model geometry (right) for SCM. Bottom: Cartilage segmentation (left) and model geometry (right) for FEM. ..... 95
Figure 3.3. Visual comparison of mesh resolution of FEM (left) and SCM (right) in the contact region. ..... 95
Figure 3.4. Top: loaded metacarpal (green) registered to the unloaded metacarpal (red). Bottom: unloaded trapezium (green) registered to the transformed-loaded trapezium (red). Left: initial position. Right: aligned position. ..... 96
Figure 3.5. Segmentation of contact area directly from the loaded image. ..... 96
Figure 3.6. MRI image of Subject 3 with osteophyte marked by the red circle. ..... 97
Figure 3.7. Contact pressure distribution on the trapezium cartilage surface. ..... 98

Figure 3.8. Peak pressures computed from SCMU, SCMV, FEML and FEMQ for all three subjects. FEM PPs were consistently higher than SCM PPs. ..... 99
Figure 3.9. Pressure distribution inside the cartilage viewed from a cutting plane for all three subjects. Top: metacarpal cartilage. Bottom: trapezium cartilage. ..... 100
Figure 3.10. Contact forces computed from SCMU, SCMV, FEML and FEMQ for all three subjects. ..... 101

## Motivation

Thumb carpometacarpal (CMC) osteoarthritis (OA) has long been a major health problem for postmenopausal women. Thumb CMC OA has a profound impact on patients' quality of life as they lose the ability to perform routine daily living activities such as holding keys and opening jars. The etiology of thumb CMC OA remains unclear and treatment outcomes are still less than satisfactory. In addition there hasn't been a well-developed system for the prevention, early detection and intervention of thumb CMC OA. As the average age of the worldwide population increases, the number of people affected by thumb CMC OA and the related healthcare resource consumption will rapidly increase.

The motivation of this study is to investigate the etiology of thumb CMC OA based on the in vivo thumb CMC joint contact mechanics. It has been widely accepted that the contact distribution on the articular surface can directly regulate the cartilage conditions. Highly concentrated contact stresses exerted on the cartilage are more likely to damage the cartilage integrity and initiate OA. The thumb CMC joint is partially incongruent with limited bony stability. Laxity of the stabilizing ligaments and the lack of intrinsic muscular strength can potentially lead to unstable joint loading and cause detrimental contact conditions. Therefore understanding the contact pattern of the normal and degenerated thumb CMC joints can shed light onto the thumb CMC OA etiology and provide guidance for developing diagnosis and treatment techniques.

Two studies are presented in this thesis. The first study (Chapter 2)compares the in vivo thumb CMC joint contact mechanics between four males and four females. The substantially higher risk of thumb CMC OA in females indicates potential gender differences in the joint mechanics

conditions. Previous studies have shown that female thumb CMC joints are less congruent, and it is well accepted that females tend to have less muscular strength than males under similar conditions. Therefore, different contact patterns between males and females in normal and OA thumb CMC joints are expected and may help better understand the mechanism of thumb CMC OA development from a mechanical prospective.

The second study (Chapter 3) compares the thumb CMC joint contact mechanics data computed from two different modeling methods. The first one is finite element modeling (FEM), which is commonly accepted as the gold standard as it tends to provide more accurate results. However the time-consuming and labor-intensive analysis procedure hinders the application of FEM in clinical practice. The second method is surface-based contact modeling (SCM), which uses a simplified analysis procedure that greatly shortens the model building and analysis time. The time efficiency of SMC makes it more viable for clinical application, but the accuracy of SCM is somewhat of a concern due to the simplified contact rule. Therefore this chapter compares the contact mechanics data obtained from FEM and SCM, and evaluates the accuracy of SCM for clinical practice. A time efficient procedure to assess the patients' thumb CMC joint contact may be an effective tool for early diagnosis of thumb CMC OA and may help to evaluate the efficacy of the thumb CMC OA treatment techniques.

# 1 Background

It has been widely accepted that hand is capable of the most complex motor functions,[1] as it takes up even larger cerebral cortex motor area than the total of trunk, hip, knee, ankle and toes. Among all the five digits, the thumb declares its independence by being the only finger capable to oppose each of the other four digits. The opposable thumb with increased length relative to the other digits has been a signature feature of primates with advanced hand dexterity such as higher apes.[2] The thumb opposition is the key component to perform power grip and pinch, and therefore plays an important role in the hand function of humans. Unlike the other four digits, the thumb only has two phalanges (first and second phalanges) and 3 articular joints (carpometacarpal, metacarpophalangeal and interphalangeal joints). The thumb carpometacarpal (CMC) joint, with its unique saddle shaped articular surface, is the primary joint responsible for generating opposition.[3] However, due to its frequent exposure to repetitive loading and the lack of osseous stability, the thumb CMC joint is very commonly affected by osteoarthritis (OA).[4]

## 1.1 Anatomy

The thumb CMC complex was first described as a "saddle joint" by Fick,[5] as the articular surfaces are made up of two opposing saddles with their axes perpendicular to each other (Figure 1.1). The thumb CMC joint has also been described as a universal joint.[3] The thumb CMC joint structure has two primary degrees-of-freedom and allows for flexion/extension and abduction/adduction, which can be combined to form more complex movements such as circumduction and opposition.[6] Due to ligament laxity there is also the possibility of some axial rotation of the metacarpal with respect to the trapezium.[6, 7]

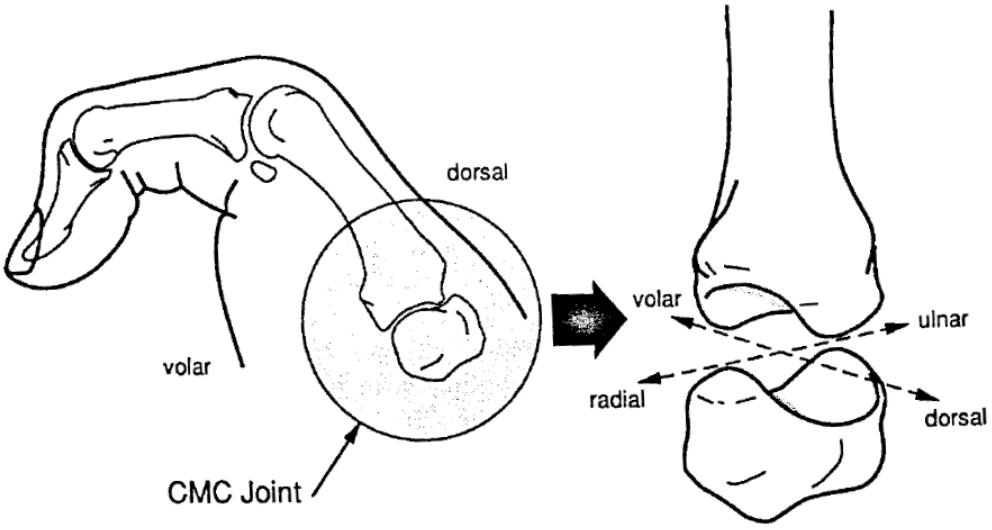


Figure 1.1. Left: location of the thumb CMC joint; right: saddle-shaped articular surfaces and perpendicular primary axes. Reprinted from The Journal of Biomechanics, Volume 25, Ateshian, G.A., Rosenwasser, M.P., and Mow, V.C., Curvature characteristics and congruence of the thumb carpometacarpal joint: differences between female and male joints, Pages 591-607, Copyright (1992), with permission from Elsevier.

## 1.2 Bones of the Thumb Basal Joint

Although the thumb CMC joint generally refers to the articulation between trapezium and metacarpal, the basal thumb contains four interactive trapezial articulations: the trapeziometacarpal (thumb CMC), scaphotrapezial, trapeziotrapezoid, and trapezium-second metacarpal articulations (Figure 1.2). The thumb CMC and scaphotrapezial joints align with the thumb compression axis,[8] and therefore are most frequently affected by radiographically-diagnosed degeneration diseases.[9, 10]

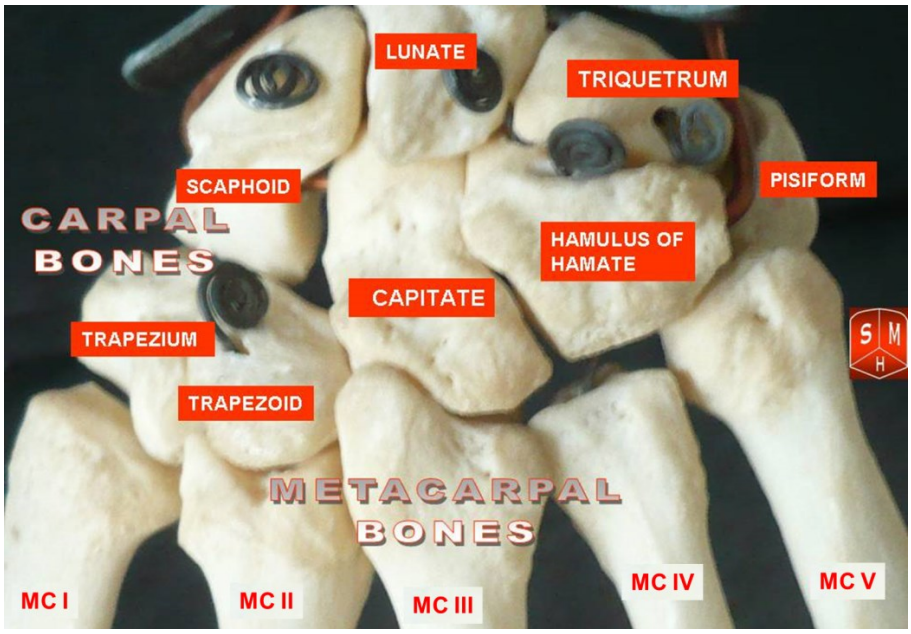


Figure 1.2. The bones articulating with trapezium include first and second metacarpal (MC I and MC II), trapezoid and scaphoid. Reprinted from http://commons.wikimedia.org/wiki/File:Carpus.jpg with modifications.

## 1.3 Muscles and Ligaments

Due to the unique shallow saddle architecture, the thumb CMC joint has limited intrinsic osseous stability, and relies primarily on the ligaments and muscles to constrain the metacarpal translation in both static and dynamic conditions.[8] The reliance on ligamentous and muscular stability greatly increases joint mobility, and allows for sufficient range-of-motion to perform opposition.[3]

The major thumb CMC joint ligaments can be divided into volar and dorsal aspects. The volar aspect contains superficial anterior oblique ligament (SAOL), deep anterior oblique ligament

(dAOL), and ulnar collateral ligament (UCL); the dorsal aspect contains dorsal radial ligament (DRL), posterior oblique ligament (POL) and intermetacarpal ligament (IML) (Figure 1.3).[11] Controversy remains on identifying the primary stabilizer of thumb CMC joint,[8] while the two most widely studied ligaments are SAOL and DRL. The SAOL originates from the trapezium palmar tubercle and inserts into the ulnar articular margin of the metacarpal base, and is elongated and tightened during metacarpal pronation to resist abduction and extension forces.[8, 12] Prior studies have shown that SAOL degeneration and detachment closely correlate with thumb CMC joint degeneration.[12, 13] The DRL is considered as the thickest and widest ligament within the thumb CMC joint, which originates from the trapezium dorsal tubercle and inserts broadly into the dorsal edge of the metacarpal base.[11] It has been shown that sectioning of DRL caused much larger metacarpal displacement than that of SAOL and IML[14], and DRL was suggested as the primary restraint during simulated metacarpal dorsal dislocation.[15]

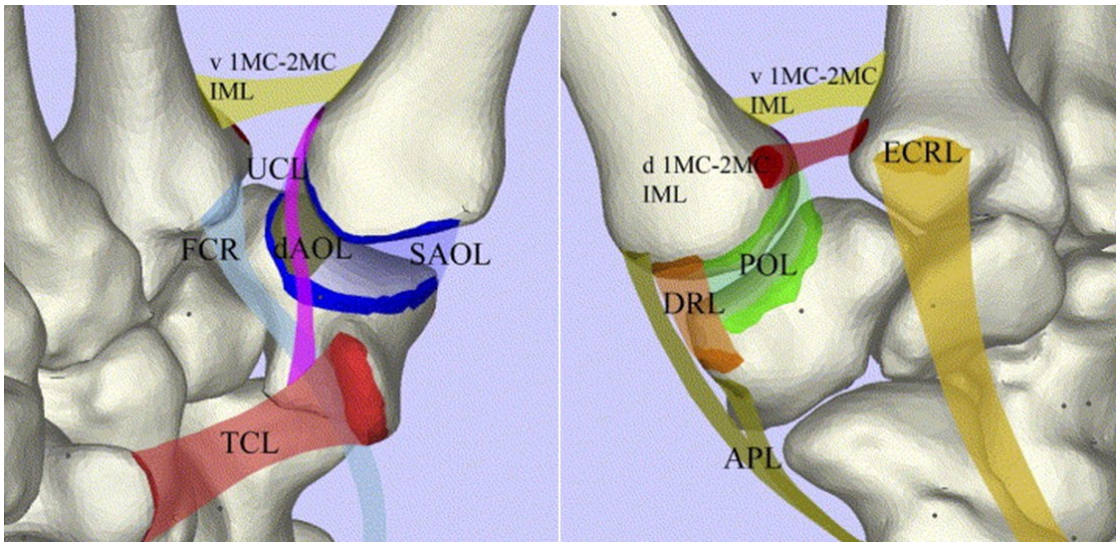


Figure 1.3. Illustration of the major ligaments and some muscles in thumb CMC joint. Left: volar view, deep anterior oblique ligament (dAOL, brown), superficial anterior oblique ligament (SAOL, dark blue), volar first metacarpal ulnar base‑second metacarpal radial base

intermetacarpal ligament (v 1MC-2MC IML, yellow), ulnar collateral ligament (UCL, purple), transverse carpal ligament (TCL, red), flexor carpi radialis (FCR, light blue). Right: dorsal view, dorsal radial ligament (DRL, orange), posterior oblique ligament (POL, green), abductor pollicis longus (APL, brown), dorsal first metacarpal ulnar base‐second metacarpal radial base intermetacarpal ligament (d 1MC-2MC IML, red), extensor carpi radialis longus (ECRL, yellow). Reprinted from The Journal of Hand Surgery, Volume 31, Nanno M., Buford W.L. Jr., Patterson R.M., Andersen C.R., Viegas S.F., Three-dimensional analysis of the ligamentous attachments of the first carpometacarpal joint, Pages 1160‐1170, Copyright (2006), with permission from Elsevier.

There are nine major muscles involved in the muscular stabilization of thumb CMC joint. The volar muscle group includes the abductor pollicis brevis, flexor carpi radialis (FCR), opponens pollicis, flexor pollicis longus, and the adductor pollicis. The dorsal muscle group includes abductor pollicis longus (APL), extensor carpi radialis longus (ECRL), extensor pollicis longus, and first dorsal interosseous muscle (Figure 1.3). These nine muscles together provide the dynamic stability of thumb CMC joint.[3] The APL inserts into the thumb metacarpal base, and is believed to cause metacarpal dorsal subluxation with insufficient ligamentous stability.[8]

## 1.4 Thumb CMC Joint Osteoarthritis

Our daily living activities such as typing, using keys, turning door knobs, and opening jars or bottles require repetitive use of the thumb. The thumb CMC joint is the primary load-bearing joint during pinch and grasp. It can experience compression force up to 12 fold of the external applied force at the fingertip during a tip pinch. While performing strong grasp, the joint contact

forces can reach 1000N.[16] Tendon forces may rise up to 300N during strong key pinch and may exceed 700N with a strong power grip.[16] Being exposed to such large loads, together with the relatively mobile bony structure, the thumb CMC joint may be frequently overloaded, likely leading to its high incidence of osteoarthritis (OA).

### 1.4.1 Prevalence, Incidence and Impact

The thumb CMC joint is the hand joint second most commonly affected by osteoarthritis.[17, 18] About 1 in 12 men and 1 in 4 women are affected by thumb CMC OA.[8, 19, 20] The prevalence of thumb CMC OA greatly increases with age,[17, 18, 21] and is substantially higher in women. More than 50% of postmenopausal women complain of pain and strength loss at the base of the thumb.[22] A study of the Framingham offspring and community cohorts showed that within 9 years cumulatively 20% of the community developed thumb CMC OA, which was the highest incidence among all hand joints.[23] Counter-intuitively, for both genders thumb CMC OA is more likely to affect non-dominant hand.[17, 23]

Patients with thumb CMC OA suffer significant pain and stiffness at thumb base,[23] with substantial loss of strength and range of motion.[24] Performing daily-activities such as holding keys and opening jars becomes very difficult and patients will eventually need a caregiver's assistance. The collapse of the thumb will occur in advanced stages of thumb CMC OA, leading to a "swan-neck" deformation as the metacarpophalangeal joint develops hyperextension in order to compensate the inability to abduct the thumb base.[25, 26]

A growing proportion of the population is considered elderly among worldwide population as life expectancies increase. By 2030, about 20% of Americans will be over 65 years old, facing a high risk of developing thumb CMC OA as well as OA in other joints. With the high price and

poor functional outcomes of surgical operation, treatment of thumb CMC OA will become an even greater contributor to future health care costs.[19]

### 1.4.2 Staging, Diagnosis and Treatment

The Eaton staging system[27], based on the radiograph of thumb CMC joint, is commonly used to determine the stage of joint degeneration. Stage 1 shows normal articular surface and widened joint space due to the synovial fluid accumulation in joint cavity; Stage 2 shows moderate joint space narrowing and osteophyte formation of less than 2 mm; in Stage 3 OA, the thumb CMC joint displays substantial narrowing, osteophyte formation and metacarpal subluxation, but the scaphotrapezium joint remains intact; in Stage 4 OA, the thumb CMC joint space is completely deteriorated, and the degeneration of scaphotrapezium joint can also be observed (Figure 1.4).

Figure 1.4. From left to right, Eaton Stage 1 - 4 thumb CMC OA as seen on a radiograph. Reprinted from The Journal of Hand Surgery, Volume 23, Barron, O.A., Eaton, R.G., Save the trapezium: Double interposition arthroplasty for the treatment of stage IV disease of the basal joint, Pages 196-204, Copyright (1998), with permission from Elsevier.

Although Eaton staging is frequently used to describe thumb CMC OA, it doesn't not predict the symptomatic severity of the disease. In many cases, individuals with radiographically apparent thumb CMC OA will report no symptoms. In clinical settings, diagnosis of thumb CMC OA often starts with physical examination including palpation and grind test, and then confirms with radiograph.[8] The treatment of thumb CMC OA is also determined based on the severity of clinical symptoms such as pain and weakness, rather than the radiographic stage.[3]

Treatment of thumb CMC OA includes both conservative and operative procedures. Conservative treatment includes hand exercises, splinting, corticosteroids and hyaluronic acid injections, which aim to strengthen the muscles, stabilize the joint, and reduce the local inflammatory response, respectively. As for the surgical treatment, ligament reconstruction and metacarpal extension osteotomy are sometimes used for patients with less severed OA. Arthrodesis is usually chosen for younger patients with high-demand occupations, as it restores the physical strength at the cost of mobility loss. For patients with advanced thumb CMC OA, trapeziectomy is the most commonly performed procedure. Following the removal of the trapezium, tendon interposition and implants are sometimes used to fill the voids in order to prevent the loss of thumb length.

Because the surgical treatment of thumb CMC OA requires a long period of immobilization and may cause additional temporary discomfort and possible complications during recovery, non-surgical procedures are often of interest.[28] However, non-surgical procedures are only suitable for early stage thumb CMC OA, and more than 50% of the patients with Stage 2 and above thumb CMC OA will fail the non-surgical treatment and require operation.[29] Many studies have

been conducted on the efficacy of different surgical procedures, but there hasn't been any clear conclusion with regard to which option provides the best outcome.[19]

### 1.4.3 Etiology

The cause of thumb CMC OA can be both primary (intrinsic or idiopathic) and posttraumatic. So far there hasn't been any longitudinal study establishing a clear etiology of primary thumb CMC OA.[8] The Bennett fracture (intra-articular fracture of the metacarpal head) is the most common injury to thumb CMC joint, which can potential lead to secondary thumb CMC OA.[3]

One of the most commonly suggested theories for primary OA of the thumb CMC joint is ligament laxity. People with hypermobility features tend to have higher risk of thumb CMC OA,[30, 31] and a cadaveric study has showed the presence of degenerated ligaments in thumb CMC joints with advanced OA.[13] Another theory is that the lack of muscle strength or muscle imbalance will lead to insufficient dynamic stability. Hand exercise programs targeting the strengthening of the thenar muscle have long been used to treat early stage thumb CMC OA.[32]

Biochemical factors such as the hormonal environment appear to be another major aspect of thumb CMC OA etiology. The lack of estrogen in postmenopausal women has been linked to multiple pathological changes in the articular joint including the degeneration of chondrocytes[33] and inflammatory response in the synovial cavity.[34, 35] The decrease of muscular strength can also be linked to estrogen deficiency.[35] In addition, women may have a higher risk of laxity due to child birth, as an immunohistochemical analysis suggested that the binding of relaxin to volar oblique ligament could potential cause ligament laxity.[36]

Although thumb CMC joint is a non-weight bearing joint, studies have found that body mass index (BMI) was directly proportional to the prevalence of thumb CMC OA.[37, 38] Such finding

can be linked to both the mechanical and biochemical factors related to thumb CMC OA. People with higher BMI may alter their joint loading due to the elevated muscle or fat composition within the joint complex. And a higher BMI may lead to multiple changes in the local biochemical environment such as lipid circulation, insulin-like growth factors, and hormones, which could potentially induce inflammatory responses and joint degeneration.[39]

### 1.4.4 Gender Differences

It has been widely accepted that females have much higher risk of thumb CMC OA than males, while there have been many proposed theories addressing the gender differences, so far no consensus has been achieved.

Estrogen is believed to have the most significant effect on female joint conditions and OA development. However, it is still unclear whether estrogen plays a protective or detrimental role on joint conditions. Although estrogen tends to enhance muscle strength, regulate cartilage conditions and maintain synovial homeostasis, high level of estrogen is also linked to the weakness and rupture of ligaments.[34, 35, 40]

The differences in articular surface geometry between males and females have also been suggested as a possible factor related to the higher thumb CMC OA prevalence in females. Women tend to have a shallower trapezium surface and hence a less congruent thumb CMC joint. That incongruence is likely to cause higher contact stress and damage the articular cartilage.[10, 41]

In addition, the relatively lower muscle strength in females compared with males also suggests that females may be more likely to encounter a lack of dynamic stability when performing activities requiring repetitive thumb loading.

## 1.5 Thumb Carpometacarpal Joint Contact Mechanics

The biochemical environment and mechanical configuration are the two main factors related to the OA development of the thumb CMC joint. From the biochemical aspect, the corticosteroids and hyaluronic acid injection has been used to treat early stage thumb CMC OA by attempting to maintain the homeostasis of the joint. From the mechanical aspect, splinting, exercise and many surgical procedures have been developed to correct the joint mechanics. As this joint is frequently subject to a significant amount of loading, the contact pressure exerted on the articular surface can greatly affect the joint conditions.[42] It has been suggested that the contact pressure and pressure distribution play an important role in regulating and maintaining the cartilage integrity throughout the lifetime.[43] The restoration of normal joint contact is also frequently evaluated in order to determine the efficacy of different treatment procedures.[44-46]

### 1.5.1 Prior Studies

Many studies have been conducted to address different aspects of the thumb CMC joint biomechanics. The contact patterns of normal and OA thumb CMC joints, cartilage wear conditions as well as the ligamentous stabilizations have been investigated based on cadaveric models, but the mechanical factors contributing to the initiations of thumb CMC OA remain controversial.

Studies by Pellegrini et al suggested that in normal thumb CMC joint the primary contact was located on the volar aspect of the trapezium and metacarpal surfaces, while with advanced stage of OA, the contact location shifted dorsally. A similar dorsal contact shift can be reproduced by detaching the SAOL (also referred as palmar beak ligament), which indicated that SAOL may be the primary ligament to stabilize the joint.[13] Similarly, Ateshian et al also suggested that during

lateral pinch the predominant contact for both surfaces was on the volar-to-ulnar regions.[47] They also analyzed the cartilage thickness on nine specimens and found that thin cartilage was most commonly presented on the ulnar and dorsoradial aspects of the trapezium, suggesting potentially higher wear on these sites.[47] However, one could also interpret thin areas of cartilage as those not commonly loaded. In contrast, Van Brenk et al compared the effect on dorsal subluxation from sectioning different ligaments and found that sectioning the DRL resulted in much larger subluxation than any other ligament. Hence the DRL should be considered an important ligamentous stabilizer of the thumb CMC joint and should be addressed during ligament reconstruction procedures.[14]

A recent in vivo kinematics study has shown that, compared with normal thumb CMC joint, a joint with OA exhibits dorsal translation of metacarpal center of rotation during flexion and adduction, which leads to an increased metacarpal volar tilt.[48] The link between this finding and the prior cadaveric contact mechanics studies is unclear. We have found no published study addressing the *in vivo* contact mechanics of the thumb CMC joint nor its alteration related to OA development.

## 1.6 Modeling Procedures

In order to address the limitations related to the previous cadaveric studies, computational modeling is frequently used to evaluate *in vivo* joint contact mechanics. Simulated functional pinch or grasp can account for the simultaneous input of muscle and tendon forces under *in vivo* conditions, which is very difficult to replicate in cadaveric studies. In addition, the non-invasiveness and repeatability of computational modeling provide great convenience in

analyzing multiple types of trauma and pathological conditions. Finite element modeling and surface-based contact modeling are two possible computational procedures.

### 1.6.1 Finite Element Modeling

Finite element modeling (FEM) is often used to solve complex structural systems which include irregular geometries, detailed material properties and multiple loading conditions. This technique is usually considered as the gold standard and believed to have the most accurate results when including deformable contact analysis for joints. However, the mesh development and refinement rely heavily on the manual input and adjustment. Although the rapid computations of FEM software can be achieved on modern computers, FEM is still a time-consuming procedure. The basic theory of finite element modeling is to break down a complex structure into a finite number of small elements with simple geometries. Tetrahedral (Figure 1.5) and hexahedral elements are the two most commonly used element types in three dimensional structures. Each element is connected to other elements by sharing one or more common nodes. Then each element is assigned specific material properties for the element type, such as the elastic modulus and Poisson's ratio for linear isotropic elements. The next step is to define the boundary conditions, which can be either the applied loads (forces or pressure) or applied/constrained displacements. Based on the force and moment equilibrium or the principle of virtual work, element equations are assembled to generate a typically very large set of matrix equations which represents the response of the entire structural system to the applied boundary conditions. Solving the system of equations will give nodal displacements, reaction forces as well as the stresses and strains.

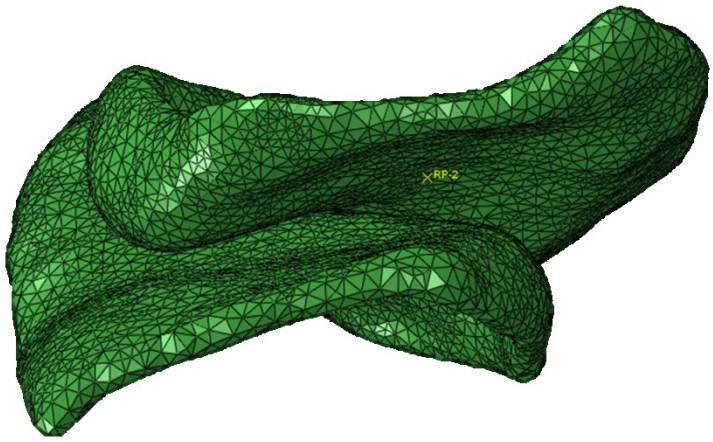


Figure 1.5. Trapezium (bottom) and metacarpal (top) tetrahedral cartilage meshes for FEM.

The polynomial equations in the matrix can be either linear or higher order, which depends upon the type of elements being chosen (e.g. linear or quadratic elements) and the additional properties related to the materials (e.g. hyperelastic materials) and interactions (e.g. sliding contact and friction). The accuracy of FEM increases with an increasing number of elements and order of the polynomial equations. Mesh refinement is often performed in the context of a mesh convergence study to assure sufficient accuracy (i.e. convergence) of the solution. When further refining the mesh yields only small variation in the solution that is within a predetermined acceptable range, the mesh is considered converged.

#### *1.6.1.1 Examples of Prior Finite Element Modeling Analyses*

Butz et al performed a COMSOL-based finite element analyze to evaluate the metacarpophalangeal (MCP) joint contact forces and stresses for gripping a pen and carrying weight.[49] The quadratic Lagrange elements were used for cartilage meshing. The stress distribution of the thumb MCP joint was computed in a two-dimensional, plane stress system. The joint and tendon forces were determined by solving force and moment equilibrium equations

in static analysis. The Young's modulus and Poisson's ratio for cartilage were assumed to be 1.12 MPa and 0.5, respectively. Cartilage was assumed to be 2 mm thick on each side of the joint with fixed contact constraints to the bone. Frictionless contact was assumed for the two articular surfaces. The simulation predicted average stress of 134 kPa at the cartilage for pen-gripping and 493kPa for weight-carrying, and the compression forces at the MCP joint were 20 N and 200 N, respectively.[49] The MCP joint apparently experienced a significantly high level of contact force but the stresses distributed on the cartilage remained relatively low. This provided basic guidance for modeling small articular joint in vivo contact mechanics. However, the cartilage material properties and thickness used in this study were not explicitly verified, nor supported by anatomical analysis. And the 2-D plane stress system may be insufficient to replicate the loading condition of the 3-D joint structure.

Gislason et al created a subject specific three-dimensional finite element model of wrist to quantify the contact mechanics of all involved joints (from finger joints to radialcarpal and ulnarcarpal joints), including the thumb MCP joint, during maximal gripping. A maximal grip strength test was performed by three subjects and the external load on was measured from the force transducer placed under each finger. The internal force on MCP joints was obtained from solving a biomechanical model.[50, 51] Bone geometry was acquired from MRI scan and joint kinematics was acquired using motion capture during the grip test. The cartilage was meshed with 10-node tetrahedral elements and assigned the material properties of 10MPa Youngs modulus and 0.4 Poisson's ratio. Ligament insertion and material properties were assigned based on previous cadaveric studies.[52, 53] Surface contact was modeled based on the hard contact algorithm and a shear force component was included to take into account the contact friction.

The results indicated that the external force applied at the thumb was much higher than those at the other fingers during maximal gripping. The calculated internal contact force for thumb MCP joint well exceeded 400N for all the subjects. FEM showed that primary contact stress was exerted on the radial aspect of the carpal bones and more than 80% of the force was transduced through radius.[50] This study primarily focused on the stress experienced by bone as an load-bearing entity. Although MCP joint reaction forces were calculated, the stress distribution on the articular cartilage was not explicitly addressed.

Previous investigations on hand and wrist joint mechanics using FEM were able to take into account various aspects including the ligament and tendon forces as well as the external loads and moment angles. But the actual stress distribution on the articular surface has not been well addressed. We have not found any study specifically applying FEM on the thumb CMC joint contact mechanics.

### 1.6.2 Surface-Based Contact Modeling

Surface-Based Contact Modeling (SCM) has been used as a simplified computational procedure. Instead of performing analysis of the full cartilage volume, two or more bilinear contact surfaces were constructed to represent the articular cartilage surfaces that are opposed according to boundary conditions. The interactions between the surfaces are determined based on a specific contact rule (e.g. linear or non-linear) (Figure 1.6).

For the articulation between two or more joint surfaces, a general 3-D quasi-static algorithm was developed by Kwak et al[51] and implemented in a general framework software, Joint_Model. The articular surfaces are assumed to be rigid and the contact forces and pressures are calculated based on the overlap of the two surfaces. The contact area is determined by the overlapping

region. Local strain is calculated by the local interpenetration and cartilage thickness. Local pressure is determined from the local strain and the applied effective cartilage relaxation modulus. Contact force is calculated by integrating the local pressure with respect to the contact area.[51]

#### *1.6.2.1 Examples of Prior Surface-based Contact Modeling Analyses*

SCM was first applied and validated by Kwak et al on modeling the patellofemoral joint of six cadaver specimens. The model was constructed based on the specimen-specific bone and articular cartilage geometries, ligament and tendon insertions as well as muscle line of force. The modeling results (medial, proximal and anterior translations, flexion, tilt and internal rotation) all obtained sufficient accuracy when compared to the experimental data.[51]

Pillai et al applied SCM on radioscaphoid, radiolunate, and scaphoidlunate articulations of four cadaveric specimens during light grasp.[52] The subject specific model geometry was obtained from MRI scan and the joint kinematic transformations were acquired by image registration to a functionally loaded MRI scan. The linear contact rule was applied and the effective cartilage relaxation modulus was assumed to be 4 MPa. Contact area, force, peak and average contact pressure were computed for each articulation in each subject. The obtained contact parameters showed reasonably good consistency compared to previous cadaveric studies, and was validated in later studies,[53-55] which indicated potential application of SCM on modeling small joints.[52]

Figure 1.6. Triangular bone surfaces (yellow) and bilinear cartilage surfaces (white) for trapezium and metacarpal for SCM

Compared with FEM, the main advantage of SCM is that model building is much less labor intensive and that it can generate the solutions much more quickly by applying the first order contact rule to the surfaces. The main disadvantages are that SCM is a low order solution (approximation) and doesn't account for the stresses and strains inside of the contacting body. A study by Johnson et al compared SCM and FEM for modeling in vivo radiolunate and radioscaphoid joint contact mechanics in order to evaluate the effect of wrist injuries and the efficacy of surgical repairs. The model geometry and kinematic transformations were obtained using the same method established by Pillai et al.[52] The contact parameters computed from SCM showed good agreement with that from FEM. The contact areas obtained from both modeling procedures matched well with the direct contact areas measured from the loaded MRI, which suggested the possibility of SCM application for clinical evaluation.[56]

## 1.7 Conclusion and Motivations

Thumb CMC OA affects a large percentage of the population and has a great impact on patients' quality of life. The etiology of thumb CMC OA remains unclear, which greatly hinders the development of early diagnosis and intervention techniques. Thumb CMC OA has disproportionally high prevalence in postmenopausal women. Understanding the mechanism related to such substantial gender differences and aging effects may provide great insights into the etiology. The contact pressure distribution on the articular cartilage surface plays a major role in regulating cartilage conditions. Alteration of contact mechanics can be an important indication of potential joint degeneration and OA development. A time-efficient tool to evaluate joint contact mechanics is important for research and may be beneficial for clinical practice. Thus, SCM may potentially be used for evaluating thumb CMC OA risk and detecting OA onset, as well as for assessing the treatment outcomes.

Therefore, the objectives of this work are to quantitatively compare the in vivo thumb CMC joint contact mechanics between males and females, and to evaluate the efficiency and accuracy of surface-based contact modeling of the thumb CMC joint, compared to finite element modeling, for potential clinical applications.

## 1.8 Reference

[1] Simpson DC. The functioning hand, the human advantage. Journal of the Royal College of Surgeons of Edinburgh. 1976;21:329-40.

[2] Moya-Sola S, Kohler M, Rook L. Evidence of hominid-like precision grip capability in the hand of the Miocene ape Oreopithecus. Proceedings of the National Academy of Sciences of the United States of America. 1999;96:313-7.

[3] Van Heest AE, Kallemeier P. Thumb carpal metacarpal arthritis. The Journal of the American Academy of Orthopaedic Surgeons. 2008;16:140-51.

[4] Brunelli GR. Stability in the first carpometacarpal joint. In: Peter Brüser AG, editor. Finger Bone and Joint Injuries1999.

[5] Fick A. Die gelenke mit sattel formigen flach, in Winter Cf. Zeitschrift fur Rationelle Medicin. 1854;Heidelberg, Germany: Adademische Verlagshandlung, 1854
314-21.

[6] Cooney WP, 3rd, Lucca MJ, Chao EY, Linscheid RL. The kinesiology of the thumb trapeziometacarpal joint. The Journal of bone and joint surgery American volume. 1981;63:1371-81.

[7] Goubier JN, Devun L, Mitton D, Lavaste F, Papadogeorgou E. Normal range-of-motion of trapeziometacarpal joint. Chirurgie de la main. 2009;28:297-300.

[8] Barron OA, Glickel SZ, Eaton RG. Basal joint arthritis of the thumb. The Journal of the American Academy of Orthopaedic Surgeons. 2000;8:314-23.

[9] North ER, Eaton RG. Degenerative joint disease of the trapezium: a comparative radiographic and anatomic study. The Journal of hand surgery. 1983;8:160-6.

[10] North ER, Rutledge WM. The trapezium-thumb metacarpal joint: the relationship of joint shape and degenerative joint disease. The Hand. 1983;15:201-6.

[11] Cardoso FN, Kim HJ, Albertotti F, Botte MJ, Resnick D, Chung CB. Imaging the ligaments of the trapeziometacarpal joint: MRI compared with MR arthrography in cadaveric specimens. AJR American journal of roentgenology. 2009;192:W13-9.

[12] Doerschuk SH, Hicks DG, Chinchilli VM, Pellegrini VD, Jr. Histopathology of the palmar beak ligament in trapeziometacarpal osteoarthritis. The Journal of hand surgery. 1999;24:496-504.

[13] Pellegrini VD, Jr., Olcott CW, Hollenberg G. Contact patterns in the trapeziometacarpal joint: the role of the palmar beak ligament. The Journal of hand surgery. 1993;18:238-44.

[14] Van Brenk B, Richards RR, Mackay MB, Boynton EL. A biomechanical assessment of ligaments preventing dorsoradial subluxation of the trapeziometacarpal joint. The Journal of hand surgery. 1998;23:607-11.

[15] Strauch RJ, Behrman MJ, Rosenwasser MP. Acute dislocation of the carpometacarpal joint of the thumb: an anatomic and cadaver study. The Journal of hand surgery. 1994;19:93-8.

[16] Cooney WP, 3rd, Chao EY. Biomechanical analysis of static forces in the thumb during hand function. The Journal of bone and joint surgery American volume. 1977;59:27-36.

[17] Wilder FV, Barrett JP, Farina EJ. Joint-specific prevalence of osteoarthritis of the hand. Osteoarthritis and cartilage / OARS, Osteoarthritis Research Society. 2006;14:953-7.

[18] Dahaghin S, Bierma-Zeinstra SM, Ginai AZ, Pols HA, Hazes JM, Koes BW. Prevalence and pattern of radiographic hand osteoarthritis and association with pain and disability (the Rotterdam study). Ann Rheum Dis. 2005;64:682-7.

[19] Martou G, Veltri K, Thoma A. Surgical treatment of osteoarthritis of the carpometacarpal joint of the thumb: a systematic review. Plast Reconstr Surg. 2004;114:421-32.

[20] Shuler MS, Luria S, Trumble TE. Basal joint arthritis of the thumb. The Journal of the American Academy of Orthopaedic Surgeons. 2008;16:418-23.

[21] Dillon CF, Hirsch R, Rasch EK, Gu Q. Symptomatic hand osteoarthritis in the United States: prevalence and functional impairment estimates from the third U.S. National Health and Nutrition Examination Survey, 1991-1994. American journal of physical medicine & rehabilitation / Association of Academic Physiatrists. 2007;86:12-21.

[22] Armstrong AL, Hunter JB, Davis TR. The prevalence of degenerative arthritis of the base of the thumb in post-menopausal women. J Hand Surg Br. 1994;19:340-1.

[23] Haugen IK, Englund M, Aliabadi P, Niu J, Clancy M, Kvien TK, et al. Prevalence, incidence and progression of hand osteoarthritis in the general population: the Framingham Osteoarthritis Study. Ann Rheum Dis. 2011;70:1581-6.

[24] Dias R, Chandrasenan J, Rajaratnam V, Burke FD. Basal thumb arthritis. Postgrad Med J. 2007;83:40-3.

[25] Burton RI, Pellegrini VD, Jr. Surgical management of basal joint arthritis of the thumb. Part II. Ligament reconstruction with tendon interposition arthroplasty. The Journal of hand surgery. 1986;11:324-32.

[26] Swanson AB. Disabling arthritis at the base of the thumb: treatment by resection of the trapezium and flexible (silicone) implant arthroplasty. The Journal of bone and joint surgery American volume. 1972;54:456-71.

[27] Eaton RG, Glickel SZ. Trapeziometacarpal osteoarthritis. Staging as a rationale for treatment. Hand clinics. 1987;3:455-71.

[28] Berggren M, Joost-Davidsson A, Lindstrand J, Nylander G, Povlsen B. Reduction in the need for operation after conservative treatment of osteoarthritis of the first carpometacarpal joint: a seven year prospective study. Scandinavian journal of plastic and reconstructive surgery and hand surgery / Nordisk plastikkirurgisk forening [and] Nordisk klubb for handkirurgi. 2001;35:415-7.

[29] Day CS, Gelberman R, Patel AA, Vogt MT, Ditsios K, Boyer MI. Basal joint osteoarthritis of the thumb: a prospective trial of steroid injection and splinting. The Journal of hand surgery. 2004;29:247-51.

[30] Gamble JG, Mochizuki C, Rinsky LA. Trapeziometacarpal abnormalities in Ehlers-Danlos syndrome. The Journal of hand surgery. 1989;14:89-94.

[31] Jonsson H, Valtysdottir ST, Kjartansson O, Brekkan A. Hypermobility associated with osteoarthritis of the thumb base: a clinical and radiological subset of hand osteoarthritis. Ann Rheum Dis. 1996;55:540-3.

[32] O'Brien VH, Giveans MR. Effects of a dynamic stability approach in conservative intervention of the carpometacarpal joint of the thumb: a retrospective study. Journal of hand therapy : official journal of the American Society of Hand Therapists. 2013;26:44-51; quiz 2.

[33] Karsdal MA, Bay-Jensen AC, Henriksen K, Christiansen C. The pathogenesis of osteoarthritis involves bone, cartilage and synovial inflammation: may estrogen be a magic bullet? Menopause international. 2012;18:139-46.

[34] Martin-Millan M, Castaneda S. Estrogens, osteoarthritis and inflammation. Joint, bone, spine : revue du rhumatisme. 2013.

[35] Roman-Blas JA, Castaneda S, Largo R, Herrero-Beaumont G. Osteoarthritis associated with estrogen deficiency. Arthritis Res Ther. 2009;11:241.

[36] Lubahn J, Ivance D, Konieczko E, Cooney T. Immunohistochemical detection of relaxin binding to the volar oblique ligament. The Journal of hand surgery. 2006;31:80-4.

[37] Haara MM, Heliovaara M, Kroger H, Arokoski JP, Manninen P, Karkkainen A, et al. Osteoarthritis in the carpometacarpal joint of the thumb. Prevalence and associations with disability and mortality. The Journal of bone and joint surgery American volume. 2004;86-A:1452-7.

[38] Kwok WY, Kloppenburg M, Rosendaal FR, van Meurs JB, Hofman A, Bierma-Zeinstra SM. Erosive hand osteoarthritis: its prevalence and clinical impact in the general population and symptomatic hand osteoarthritis. Ann Rheum Dis. 2011;70:1238-42.

[39] Walker K, Fletcher O, Johnson N, Coupland B, McCormack VA, Folkerd E, et al. Premenopausal mammographic density in relation to cyclic variations in endogenous sex hormone levels, prolactin, and insulin-like growth factors. Cancer Res. 2009;69:6490-9.

[40] Liu SH, Al-Shaikh RA, Panossian V, Finerman GA, Lane JM. Estrogen affects the cellular metabolism of the anterior cruciate ligament. A potential explanation for female athletic injury. The American journal of sports medicine. 1997;25:704-9.

[41] Ateshian GA, Rosenwasser MP, Mow VC. Curvature characteristics and congruence of the thumb carpometacarpal joint: differences between female and male joints. J Biomech. 1992;25:591-607.

[42] Shi Q, Hashizume H, Inoue H, Miyake T, Nagayama N. Finite element analysis of pathogenesis of osteoarthritis in the first carpometacarpal joint. Acta medica Okayama. 1995;49:43-51.

[43] Andriacchi TP, Mundermann A, Smith RL, Alexander EJ, Dyrby CO, Koo S. A framework for the in vivo pathomechanics of osteoarthritis at the knee. Ann Biomed Eng. 2004;32:447-57.

[44] Stephen JM, Kaider D, Lumpaopong P, Deehan DJ, Amis AA. The Effect of Femoral Tunnel Position and Graft Tension on Patellar Contact Mechanics and Kinematics After Medial Patellofemoral Ligament Reconstruction. The American journal of sports medicine. 2013.

[45] Johnson JE, Lee P, McIff TE, Toby EB, Fischer KJ. Effectiveness of surgical reconstruction to restore radiocarpal joint mechanics after scapholunate ligament injury: an in vivo modeling study. J Biomech. 2013;46:1548-53.

[46] McCarthy MM, Tucker S, Nguyen JT, Green DW, Imhauser CW, Cordasco FA. Contact stress and kinematic analysis of all-epiphyseal and over-the-top pediatric reconstruction techniques for the anterior cruciate ligament. The American journal of sports medicine. 2013;41:1330-9.

[47] Ateshian GA, Ark JW, Rosenwasser MP, Pawluk RJ, Soslowsky LJ, Mow VC. Contact areas in the thumb carpometacarpal joint. Journal of orthopaedic research : official publication of the Orthopaedic Research Society. 1995;13:450-8.

[48] Miura T, Ohe T, Masuko T. Comparative in vivo kinematic analysis of normal and osteoarthritic trapeziometacarpal joints. The Journal of hand surgery. 2004;29:252-7.

[49] Butz KD, Merrell G, Nauman EA. A biomechanical analysis of finger joint forces and stresses developed during common daily activities. Comput Methods Biomech Biomed Engin. 2012;15:131-40.

[50] Fowler NK, Nicol AC. Interphalangeal joint and tendon forces: normal model and biomechanical consequences of surgical reconstruction. J Biomech. 2000;33:1055-62.

[51] Fowler NK, Nicol AC. Functional and biomechanical assessment of the normal and rheumatoid hand. Clin Biomech (Bristol, Avon). 2001;16:660-6.

[52] Berger RA. The ligaments of the wrist. A current overview of anatomy with considerations of their potential functions. Hand clinics. 1997;13:63-82.

[53] Berger RA, Imeada T, Berglund L, An KN. Constraint and material properties of the subregions of the scapholunate interosseous ligament. The Journal of hand surgery. 1999;24:953-62.

[54] Gislason MK, Nash DH, Nicol A, Kanellopoulos A, Bransby-Zachary M, Hems T, et al. A three-dimensional finite element model of maximal grip loading in the human wrist. Proceedings of the Institution of Mechanical Engineers Part H, Journal of engineering in medicine. 2009;223:849-61.

[55] Kwak SD, Blankevoort L, Ateshian GA. A Mathematical Formulation for 3D Quasi-Static Multibody Models of Diarthrodial Joints. Comput Methods Biomech Biomed Engin. 2000;3:41-64.

[56] Pillai RR, Thoomukuntla B, Ateshian GA, Fischer KJ. MRI-based modeling for evaluation of in vivo contact mechanics in the human wrist during active light grasp. J Biomech. 2007;40:2781-7.

[57] Thoomukuntla BR, Mciff TE, Ateshian GA, Bilgen M, Toby EB, Fischer KJ. Preliminary Validation f Mri-Based Modeling for Evaluation of Joint Mechanics. J Musculosketeletal Res. 2008;11:161-71.

[58] Johnson JE, McIff TE, Lee P, Toby EB, Fischer KJ. Validation of radiocarpal joint contact models based on images from a clinical MRI scanner. Comput Methods Biomech Biomed Engin. 2012.

[59] Fischer KJ, Johnson JE, Waller AJ, McIff TE, Toby EB, Bilgen M. MRI-based modeling for radiocarpal joint mechanics: validation criteria and results for four specimen-specific models. Journal of biomechanical engineering. 2011;133:101004.

[60] Johnson JE. Computationally Efficient MRI-based Surface Contact Modeling as a Tool to Evaluate Joint. Injuries and Outcomes of Surgical Interventions. 2013.

This page left intentionally blank.

# 2 Gender Differences and Aging Effects of *In Vivo* Thumb Carpometacarpal Joint Contact Mechanics

This page left intentionally blank.

Submitted to Journal of Biomechanical Engineering

# Gender Differences and Aging Effects of *In Vivo* Thumb Carpometacarpal Joint Contact Mechanics

**Qi Zheng**
Department of Bioengineering, University of Kansas
1530 West 15th Street, 3138 Learned Hall, Lawrence, KS, 66045
qzheng@ku.edu

**Phil Lee**
Hoglund Brain Imaging Center, University of Kansas Medical Center
3901 Rainbow Boulevard, Kansas City, KS, 66160
plee2@kumc.edu

**Terence E. McIff**
Department of Orthopedic Surgery, University of Kansas Medical Center
3901 Rainbow Boulevard, Kansas City, KS, 66160
tmciff@kumc.edu

**E. Bruce Toby**
Department of Orthopedic Surgery, University of Kansas Medical Center
University of Kansas Medical Center, 3901 Rainbow Boulevard, Kansas City, KS, 66160
btoby@kumc.edu

**Kenneth J. Fischer**[1]
Department of Mechanical Engineering, University of Kansas
1530 West 15th Street, 3138 Learned Hall, Lawrence, KS, 66045
Phone: 785-864-2994
Fax: 785-864-5254
fischer@ku.edu
ASME member since 1995

[1] Corresponding author

This page left intentionally blank.

## 2.1 Abstract

Osteoarthritis (OA) of the thumb carpometacarpal (CMC) joint has much higher prevalence in women than in men, and greatly increases with age. The purpose of this preliminary study is to compare the in vivo thumb CMC joint contact mechanics between males and females. Finite element models were constructed for four males and four females based on MRI imaging during functional loading. A trend of increasing peak contact pressure with age was seen for females but not for males. Contact region size and location showed different patterns between males and females as well, indicating gender differences in joint contact mechanics that are likely related to the high thumb CMC OA risk in older women.

## 2.2 Introduction

The thumb carpometacarpal (CMC) joint is an essential joint in the hand for performing pinch and grasp. It is a primary load bearing joint which can be subject to 12 times of the force exerted at the fingertip during a simple tip pinch [1]. Many routine tasks of daily living, such as writing, typing and texting require repetitive use of the thumb. Unfortunately, the thumb CMC joint has the second highest prevalence of osteoarthritis (OA) among all hand joints [2, 3]. Thumb CMC OA affects 1 in 12 men and 1 in 4 women [4, 5].

The prevalence of thumb CMC OA shows substantial gender differences and aging effects, and is predominately found in postmenopausal women [3, 6]. The etiology of this disease remains unclear, although it is believed that it can be initiated by both mechanical factors (e.g. lack of ligamentous stability, muscular stability, or joint incongruity) and/or biochemical factors (e.g. hormonal environment or inflammatory response) [4].

Previous studies have looked at different aspects of the thumb CMC joint biomechanics, including the kinematics and joint contact mechanics [7-10], however, the contact patterns in the normal *in vivo* joint and OA thumb CMC joint remain undetermined. Although it's strongly suggested that ligament laxity is likely an important factor contributing to the thumb CMC OA development [4], controversy remains on identifying the primary ligamentous stabilizer of this joint [9, 11, 12]. So far we have found no published data on *in vivo* thumb CMC joint contact mechanics. Since the contact pressure distribution can greatly affect the cartilage condition [13], better understanding of the *in vivo* thumb CMC joint contact mechanics can bring insight into the thumb CMC OA etiology and provide guidance to improve diagnosis and treatment. Therefore the objective of this preliminary study is to quantitatively investigate the *in vivo* thumb CMC joint contact mechanics and the differences related to gender and aging effects.

## 2.3 Methods

### 2.3.1 Subjects and MRI Scan

Eight subjects were divided into male (4 males, age 26-56) and female (4 females, age 33-69) groups (study approved by IRB). No subjects reported previous injury or diagnosis of OA to the thumb CMC joint. Each subject had one hand scanned using a 3T clinical MRI system (Siemens Skyra, Siemens, USA) with a dual echo steady state (DESS) sequence. Two sets of images were obtained for each hand. First, the relaxed hand was placed flat in a palm-down position and scanned at a high resolution (0.22 mm×0.2 mm in-plane pixel size, 0.5 mm slice thickness, designated the unloaded image set, Figure. 2.1); then the same hand was used to grip a 25 mm diameter air-pressurized tube (initial pressure = 3.0 psi = 20.7 kPa) and scanned at a relatively

lower resolution (0.31 mm×0.31 mm in-plane pixel size, 1.0 mm slice thickness, designated the loaded image set, Figure. 2.2A-B). The reduced resolution shortened the scan time in order to minimize subject fatigue and motion artifact. Each subject was asked to wear a wrist brace during the loaded scan to ensure a consistent gripping position. Visual feedback (Figure. 2.2C) was provided to the subjects to ensure that each time the tube was gripped to and held at a consistent target pressure (3.125 psi = 21.5 kPa).

### 2.3.2 Modeling Geometry

The cartilage of the trapezium and of the first metacarpal was segmented from the unloaded image set using ScanIP (Simpleware Ltd, Exeter, UK). A 3-D linear tetrahedral volume mesh was constructed from each segmented cartilage volume using the ScanIP/FE module (Figure. 2.3). In addition to the initial meshing, two more mesh refinements were performed sequentially, each with higher mesh density than the previous one, to assure mesh convergence.

### 2.3.3 Kinematic Transformation

Image registration was performed to obtain the transformation to the loaded joint configuration during the applied light grasp. Based on the assumption that the bones were rigid during the loading, the registration was performed on the isolated bones. The trapezium and metacarpal bones were segmented without cartilage and isolated on a black background from both the unloaded and the loaded image sets (Figure. 2.4). Analyze 5.0 voxel-based registration was used to determine the transformation. The metacarpal was used as the reference. First the loaded metacarpal was registered to the unloaded metacarpal in order to align the coordinate of the loaded image set to that of the unloaded image set. Then the loaded trapezium was transformed into the unloaded coordinate system using the obtained reference transformation. In this way the

transformed-loaded trapezium and the unloaded trapezium were compared in the same coordinate system. Finally the unloaded trapezium was registered to the transformed-loaded trapezium, which gave the joint kinematic transformation from the unloaded to the loaded configuration (Figure. 2.5).

### 2.3.4 Modeling and Verification

Finite element modeling was performed in Abaqus 6.9 (Simulia, Providence, RI) (Figure. 2.6). Cartilage was modeled as a homogeneous, isotropic, elastic solid with Young's modulus (effective relaxation modulus) of 4 MPa and Poisson's ratio of 0.2 based on previous studies [14, 15]. The obtained kinematic transformation for the trapezium was applied as a displacement boundary condition for each modeling analysis, while the metacarpal cartilage was held fixed (Figure. 2.6). Subchondral surface was assumed to be rigidly constrained by the displacement boundary conditions. The contact between the two cartilage volumes was assumed to be frictionless with finite sliding [16]. Contact force (CF) and contact area (CA), as well as peak contact pressure (PP) and average contact pressure (AP) were computed for each modeling analysis. Less than 5% variation of contact force was accepted as the mesh convergence criterion. The contact region visible on the loaded MR image set was segmented to directly measure the contact area from the loaded image, and the obtained direct contact area was compared with the contact area computed from the model in order to verify the model accuracy (Figure. 2.7) [16].

### 2.3.5 Statistical Analysis

Statistical analysis was performed in SPSS (IBM, Armonk, New York). To analyze the gender difference, contact area, force, peak and average contact pressures were compared between male and female groups using student t-test, and the f-test was used to evaluate the within group

variation. Within each gender group, linear regression with age was performed for each obtained contact measure to evaluate the aging effects for males and females separately. Linear regression with body weight (BW) and body mass index (BMI), separately, were also performed on each obtained parameter to determine the possible effects from body size. Statistical significance was defined as $p < 0.05$.

## 2.4 Results

Mesh convergence was achieved by refining the trapezium mesh from 3752 to 6655 nodes and metacarpal mesh from 3515 to 8600 nodes. Although all subjects self-reported asymptomatic, from the MRI images Subject F4 showed substantial joint space narrowing and osteophyte formation (Figure. 2.8), which indicated an advanced stage of thumb CMC OA. This is consistent with the observed phenomenon that the radiographic staging of thumb CMC OA has very poor correlation with the symptoms.

The mean value of each obtained parameter showed no apparent differences between male and female groups (all $p > 0.2$). However, the within-group variation of contact force and area were much smaller for males than for females (Figure. 2.9), and were nearly significant (f test yielded $p = 0.058$ for CF, $p = 0.051$ for CA). No apparent aging pattern was observed in the male group for any computed parameters ($p > 0.4$ for the regression analysis of all contact parameters within male group). In the female group, CF and PP showed trends of increasing with age ($p = 0.091$ for CF vs. age, $p = 0.097$ for PP vs. age) (Figure. 2.10). For both male and female group, there were no apparent effects of either BW or BMI on any of the contact parameters (within male group all contact parameters $p > 0.2$, within female group all contact parameters $p > 0.4$) (Figure. 2.10).

All the above statistics were performed with results from standard material properties for all subjects. However, Subject F4 had contact force of 80 N, which was unreasonably high for a light grasp. To account for apparent OA in this subject, the model was re-analyzed using a modulus of 2 MPa. The resulting force (40 N) was similar to the other subjects. PP and AP were also reduced to half the original values, though CA was not notably different (Table 2.1).

The contact pressure distribution for the male subjects showed both medial (M2 and M3) and volar-lateral (M1 and M4) patterns (Figure. 2.11), and the PP with medial contact (M2 and M3) were individually higher than the PP with volar-lateral contact (M1 and M4). For the first three female subjects contact was consistently located on the medial edge of both surfaces with PP located at the middle-to-volar region; while Subject F4 showed a unique dispersed contact pattern which yielded much larger contact area and force, and PP substantially shifted in the dorsal direction compared with all the other subjects (Figure. 2.11).

Contact areas computed from the modeling analysis were on average within 15% variation from the contact areas directly measured from the loaded image (Figure. 2.12), which verified the model accuracy. In addition, the regression analysis showed a significant correlation ($R^2 = 0.98$, slope = 0.93) between the modeled and direct contact areas.

## 2.5 Discussion

The poor correlation between radiographic and symptomatic thumb CMC OA often makes it difficult to detect the disease at its early radiographic stage [17]. By the time that patients start to feel the discomfort and seek treatment, the OA has typically progressed to an advanced stage, in which the primary treatment is trapeziectomy. Removal of the trapezium can achieve pain relief

of the joint, but at the cost of permanent loss of strength, thumb height, and hand opening range [18]. It also leads to a higher risk of metacarpophalangeal (MCP) joint hyperextension to compensate the loss of working space [19].

Based on the previous cadaveric studies, the observed contact force and area from the current study were all within the expected range except for Subject F4 [1]. The contact force for Subject F4 appeared to be too high for the light grasp functional task. Based on the MR image evidence, it is reasonable to believe that Subject F4 had developed advanced stage of OA, which means the cartilage material properties (Young's modulus and Poisson's ratio) may have been substantially different from other subjects with relatively normal thumb CMC joint. With advanced OA, the cartilage degeneration will lead to decreased modulus [20], then the 4 MPa effective relaxation modulus might be too high for Subject F4, which caused the unreasonably high CF. Therefore we re-evaluated the contact parameters of Subject F4 using 2 MPa as the Young's modulus. With the reduced Young's modulus, the CA remained the same while CF, PP and AP all decreased to approximately half of the original value. The reduced CF appeared more reasonable for light grasp activity and similar to CF for other subjects. However, the exact change of cartilage material properties of Subject F4 (or any other subject) cannot be obtained non-invasively, which is a general limitation of modeling normal joints and especially joints with evidence of OA development.

The thumb CMC joint is partially incongruent [21]. As a result, contact located at different regions (i.e. dorsal vs. volar and medial vs. lateral) can lead to substantially different joint loading conditions. As is indicated from the male subject group, the contact located at the lateral-volar edge appeared to be evenly distributed with a relatively larger CA and lower PP, while the

contact located at the center of the medial edge yielded lower CA and higher PP. Interestingly, such medial-edge contact pattern was consistently observed for all the female subjects. This might indicate intrinsic gender differences in joint configuration. As has been suggested in the study by Ateshian et al, the curvatures of the trapezium articular surface were fundamentally different between males and females, while the metacarpal articular surface geometry showed no significant gender differences. As a result, the articulation of the thumb CMC joint may have been substantially less congruent in females than in males [21].

In addition to the potential gender differences in the articular surface geometry and joint congruency, it is also likely that the intrinsic differences in muscular and ligamentous properties can lead to different joint stability between males and females. There have been multiple studies focusing on the gender differences in the anterior cruciate ligament (ACL). The outcomes consistently suggest that because females are likely to have less neuromuscular control and ligamentous strength, they may have higher tendency to develop instability issues under both static and dynamic conditions [22, 23]. However, so far there hasn't been any study comparing the differences of muscular and ligamentous properties specifically to the thumb CMC joint.

Another important aspect of gender differences is the hormonal environment. Estrogen can play an important role in the local synovial homeostasis and the soft tissue remodeling including both ligaments and articular cartilage [23, 24]. Studies have shown that the estrogen deficiency in postmenopausal women is closely related to the increased risk of OA development [25]. On the other hand, it has been suggested that in younger females ACL laxity significantly increases with peak levels of estrogen and progesterone during a menstrual cycle, which predisposes the joint to instability and risk of injury [26]. Therefore it is still unclear whether the female hormones,

especially estrogen, are protective or destructive to the articular joint integrity. In addition, relaxin is known to reduce ligament stiffness and high levels of relaxin during pregnancy may have long-term effects on thumb CMC joint instability and OA development [27, 28]. As the thumb CMC joint greatly relies on muscular and ligamentous stability, further studies are definitely needed to look at the hormonal effects specifically at this joint, which may correlate with the alterations in joint contact mechanics. A comprehensive understanding of thumb CMC OA from both mechanical and biochemical aspects will provide needed information to the development of prevention, early diagnosis and intervention techniques.

Previous studies suggested that BMI was directly proportional to thumb CMC OA prevalence [29, 30]. An increased BMI may lead to higher muscle and fat composition and therefore increase loading. Also changes in BMI may result in changes in local biochemical environment, leading to potential inflammatory responses causing cartilage degeneration [31]. However, in the current study the effects of either BW or BMI on joint contact mechanics was not observed from the linear regression analysis, which is likely due to the small number of subjects in each gender group.

There are several limitations in this study. The material properties were taken from the literature and not determined or estimated for each individual subject. As shown, the assumed modulus has a large direct effect on the results. The finite element analysis was performed using linear tetrahedral element for the efficiency of meshing and refinement, which may lead to a stiffer response than quadratic tetrahedrons or hexahedrons. The subchondral cartilage surface was assumed to be rigid, which may also cause a higher peak pressure since the bone deformation was not considered. The joint contact was simulated under a static condition with fixed

displacement boundary conditions, while the actual grasp activity is under the balance of muscular activity and ligamentous constraints. However, the displacement boundary conditions reflect the actual *in vivo* bone interactions. In addition, with the small number of subjects in each group, the statistical analysis may be considered inconclusive. Finally, no biochemical assays were made for this preliminary study.

## 2.6 Conclusion

This study acquired thumb CMC joint contact mechanics data which indicates gender differences potentially related to the differences in the articular surface geometry, muscular and ligamentous strength as well as the hormonal environment. Such gender differences may be closely associated with the higher risk of thumb CMC OA development in females, especially postmenopausal women. Future studies need to investigate the comprehensive effects from both mechanical and biochemical factors based on larger cohorts of subjects, in order to further understand the etiology of thumb CMC OA and provide guidance for improving prevention, diagnosis and treatment techniques.

## 2.7 Acknowledgments

We would like to acknowledge technical assistance from Allan Schmitt and Frank Hunsinger.

## 2.8 Funding

Support for the study was provided by the National Institute of Biomedical Imaging and Bioengineering of the National Institutes of Health under award R01EB008709.

## 2.9 References


[1] Cooney, W. P., 3rd, and Chao, E. Y., 1977, "Biomechanical Analysis of Static Forces in the Thumb During Hand Function," J Bone Joint Surg Am, 59(1), pp. 27-36.

[2] Haugen, I. K., Englund, M., Aliabadi, P., Niu, J., Clancy, M., Kvien, T. K., and Felson, D. T., 2011, "Prevalence, Incidence and Progression of Hand Osteoarthritis in the General Population: The Framingham Osteoarthritis Study," Ann Rheum Dis, 70(9), pp. 1581-6. 10.1136/ard.2011.150078.

[3] Dahaghin, S., Bierma-Zeinstra, S. M., Ginai, A. Z., Pols, H. A., Hazes, J. M., and Koes, B. W., 2005, "Prevalence and Pattern of Radiographic Hand Osteoarthritis and Association with Pain and Disability (the Rotterdam Study)," Ann Rheum Dis, 64(5), pp. 682-7. 10.1136/ard.2004.023564.

[4] Barron, O. A., Glickel, S. Z., and Eaton, R. G., 2000, "Basal Joint Arthritis of the Thumb," J Am Acad Orthop Surg, 8(5), pp. 314-23.

[5] Shuler, M. S., Luria, S., and Trumble, T. E., 2008, "Basal Joint Arthritis of the Thumb," J Am Acad Orthop Surg, 16(7), pp. 418-23.

[6] Armstrong, A. L., Hunter, J. B., and Davis, T. R., 1994, "The Prevalence of Degenerative Arthritis of the Base of the Thumb in Post-Menopausal Women," J Hand Surg Br, 19(3), pp. 340-1.

[7] Miura, T., Ohe, T., and Masuko, T., 2004, "Comparative in Vivo Kinematic Analysis of Normal and Osteoarthritic Trapeziometacarpal Joints," J Hand Surg Am, 29(2), pp. 252-7. 10.1016/j.jhsa.2003.11.002.

[8] Momose, T., Nakatsuchi, Y., and Saitoh, S., 1999, "Contact Area of the Trapeziometacarpal Joint," J Hand Surg Am, 24(3), pp. 491-5. 10.1053/jhsu.1999.0491.

[9] Pellegrini, V. D., Jr., Olcott, C. W., and Hollenberg, G., 1993, "Contact Patterns in the Trapeziometacarpal Joint: The Role of the Palmar Beak Ligament," J Hand Surg Am, 18(2), pp. 238-44. 10.1016/0363-5023(93)90354-6.

[10] Ateshian, G. A., Ark, J. W., Rosenwasser, M. P., Pawluk, R. J., Soslowsky, L. J., and Mow, V. C., 1995, "Contact Areas in the Thumb Carpometacarpal Joint," J Orthop Res, 13(3), pp. 450-8. 10.1002/jor.1100130320.

[11] Van Brenk, B., Richards, R. R., Mackay, M. B., and Boynton, E. L., 1998, "A Biomechanical Assessment of Ligaments Preventing Dorsoradial Subluxation of the Trapeziometacarpal Joint," J Hand Surg Am, 23(4), pp. 607-11.

[12] Cardoso, F. N., Kim, H. J., Albertotti, F., Botte, M. J., Resnick, D., and Chung, C. B., 2009, "Imaging the Ligaments of the Trapeziometacarpal Joint: Mri Compared with Mr Arthrography in Cadaveric Specimens," AJR Am J Roentgenol, 192(1), pp. W13-9. 10.2214/AJR.07.4010.

[13] Andriacchi, T. P., Mundermann, A., Smith, R. L., Alexander, E. J., Dyrby, C. O., and Koo, S., 2004, "A Framework for the in Vivo Pathomechanics of Osteoarthritis at the Knee," Ann Biomed Eng, 32(3), pp. 447-57.

[14] Kwak, S. D., Blankevoort, L., and Ateshian, G. A., 2000, "A Mathematical Formulation for 3d Quasi-Static Multibody Models of Diarthrodial Joints," Comput Methods Biomech Biomed Engin, 3(1), pp. 41-64. 10.1080/10255840008915253.

[15] Jurvelin, J. S., Buschmann, M. D., and Hunziker, E. B., 1997, "Optical and Mechanical Determination of Poisson's Ratio of Adult Bovine Humeral Articular Cartilage," J Biomech, 30(3), pp. 235-41.

[16] Johnson, J. E., Mciff, T. E., Lee, P., Toby, E. B., and Fischer, K. J., 2012, "Validation of Radiocarpal Joint Contact Models Based on Images from a Clinical Mri Scanner," Comput Methods Biomech Biomed Engin, pp. 10.1080/10255842.2012.684446.

[17] Burton, R. I., 1973, "Basal Joint Arthrosis of the Thumb," Orthop Clin North Am, 4(2), pp. 331-8.

[18] Pellegrini, V. D., Jr., Parentis, M., Judkins, A., Olmstead, J., and Olcott, C., 1996, "Extension Metacarpal Osteotomy in the Treatment of Trapeziometacarpal Osteoarthritis: A Biomechanical Study," J Hand Surg Am, 21(1), pp. 16-23. 10.1016/S0363-5023(96)80149-3.

[19] Poulter, R. J., and Davis, T. R., 2011, "Management of Hyperextension of the Metacarpophalangeal Joint in Association with Trapeziometacarpal Joint Osteoarthritis," J Hand Surg Eur Vol, 36(4), pp. 280-4. 10.1177/1753193411400359.

[20] Boschetti, F., and Peretti, G. M., 2008, "Tensile and Compressive Properties of Healthy and Osteoarthritic Human Articular Cartilage," Biorheology, 45(3-4), pp. 337-44.

[21] Ateshian, G. A., Rosenwasser, M. P., and Mow, V. C., 1992, "Curvature Characteristics and Congruence of the Thumb Carpometacarpal Joint: Differences between Female and Male Joints," J Biomech, 25(6), pp. 591-607.

[22] Hewett, T. E., Zazulak, B. T., Myer, G. D., and Ford, K. R., 2005, "A Review of Electromyographic Activation Levels, Timing Differences, and Increased Anterior Cruciate Ligament Injury Incidence in Female Athletes," Br J Sports Med, 39(6), pp. 347-50. 10.1136/bjsm.2005.018572.

[23] Slauterbeck, J. R., Hickox, J. R., Beynnon, B., and Hardy, D. M., 2006, "Anterior Cruciate Ligament Biology and Its Relationship to Injury Forces," Orthop Clin North Am, 37(4), pp. 585-91. 10.1016/j.ocl.2006.09.001.

[24] Tanamas, S. K., Wijethilake, P., Wluka, A. E., Davies-Tuck, M. L., Urquhart, D. M., Wang, Y., and Cicuttini, F. M., 2011, "Sex Hormones and Structural Changes in Osteoarthritis: A Systematic Review," Maturitas, 69(2), pp. 141-56. 10.1016/j.maturitas.2011.03.019.

[25] Martin-Millan, M., and Castaneda, S., 2013, "Estrogens, Osteoarthritis and Inflammation," Joint Bone Spine, pp. 10.1016/j.jbspin.2012.11.008.

[26] Heitz, N. A., Eisenman, P. A., Beck, C. L., and Walker, J. A., 1999, "Hormonal Changes Throughout the Menstrual Cycle and Increased Anterior Cruciate Ligament Laxity in Females," J Athl Train, 34(2), pp. 144-9.

[27] Dragoo, J. L., Lee, R. S., Benhaim, P., Finerman, G. A., and Hame, S. L., 2003, "Relaxin Receptors in the Human Female Anterior Cruciate Ligament," Am J Sports Med, 31(4), pp. 577-84.

[28] Lubahn, J., Ivance, D., Konieczko, E., and Cooney, T., 2006, "Immunohistochemical Detection of Relaxin Binding to the Volar Oblique Ligament," J Hand Surg Am, 31(1), pp. 80-4. 10.1016/j.jhsa.2005.09.012.

[29] Haara, M. M., Heliovaara, M., Kroger, H., Arokoski, J. P., Manninen, P., Karkkainen, A., Knekt, P., Impivaara, O., and Aromaa, A., 2004, "Osteoarthritis in the Carpometacarpal Joint of the Thumb. Prevalence and Associations with Disability and Mortality," J Bone Joint Surg Am, 86-A(7), pp. 1452-7.

[30] Kwok, W. Y., Kloppenburg, M., Rosendaal, F. R., Van Meurs, J. B., Hofman, A., and Bierma-Zeinstra, S. M., 2011, "Erosive Hand Osteoarthritis: Its Prevalence and Clinical Impact in the General Population and Symptomatic Hand Osteoarthritis," Ann Rheum Dis, 70(7), pp. 1238-42. 10.1136/ard.2010.143016.

[31] Walker, K., Fletcher, O., Johnson, N., Coupland, B., Mccormack, V. A., Folkerd, E., Gibson, L., Hillier, S. G., Holly, J. M., Moss, S., Dowsett, M., Peto, J., and Dos Santos Silva, I., 2009, "Premenopausal Mammographic Density in Relation to Cyclic Variations in Endogenous Sex Hormone Levels, Prolactin, and Insulin-Like Growth Factors," Cancer Res, 69(16), pp. 6490-9. 10.1158/0008-5472.CAN-09-0280.

## 2.10 Tables and Figures

Table 2.1. Contact measures for each individual subject, including Subject F4 with 2 MPa cartilage effective relaxation modulus (noted as F4r).

| Subject | Age | CF (N) | CA ($mm^2$) | PP (MPa) | AP (MPa) | BW (kg) | Height (cm) | BMI |
|---|---|---|---|---|---|---|---|---|
| **M1** | 26 | 28 | 41 | 1.6 | 0.7 | 100 | 188 | 28 |
| **M2** | 33 | 25 | 30 | 2.0 | 0.8 | 91 | 193 | 24 |
| **M3** | 35 | 32 | 35 | 2.1 | 0.9 | 141 | 185 | 41 |
| **M4** | 56 | 23 | 39 | 1.6 | 0.6 | 107 | 180 | 33 |
| **F1** | 33 | 8 | 16 | 1.1 | 0.5 | 50 | 160 | 20 |
| **F2** | 50 | 18 | 17 | 1.8 | 1.0 | 88 | 168 | 31 |
| **F3** | 60 | 39 | 23 | 2.5 | 1.5 | 63 | 157 | 25 |
| **F4** | 69 | 80 | 80 | 2.2 | 1.0 | 84 | 170 | 29 |
| **F4r** | 69 | 40 | 80 | 1.1 | 0.5 | 84 | 170 | 29 |

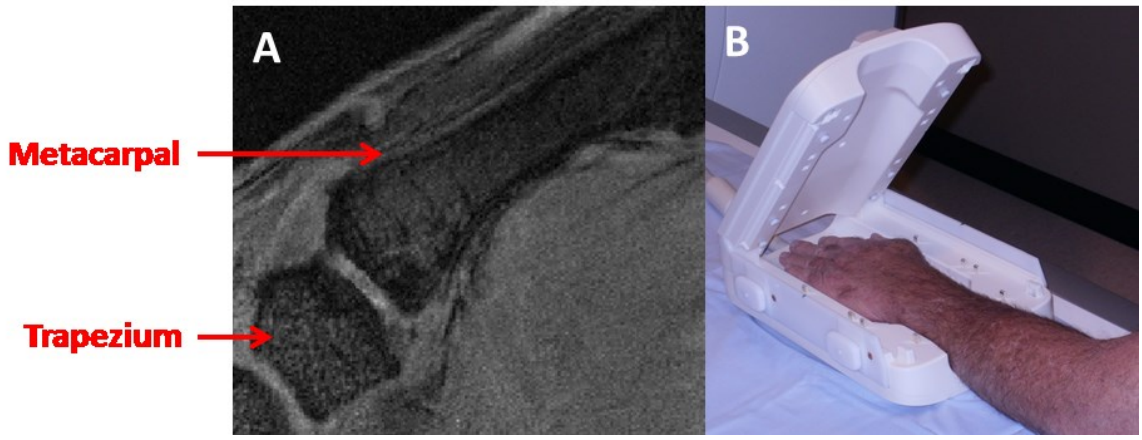


Figure 2.1. (A) The unloaded MRI image of the trapezium and metacarpal. (B) The hand position and coil for the unloaded scan.

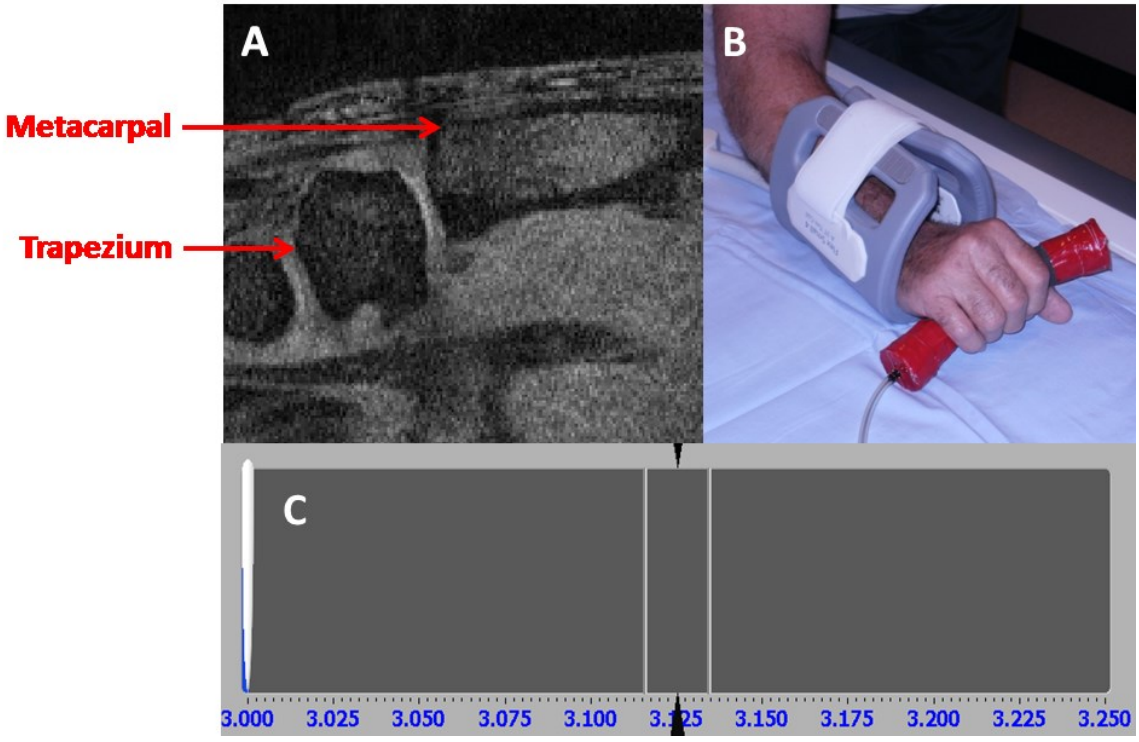


Figure 2.2. (A) The loaded MRI image of the trapezium and metacarpal. (B) The hand position and coil for the loaded scan. (C) The visual feedback for the loaded scan.

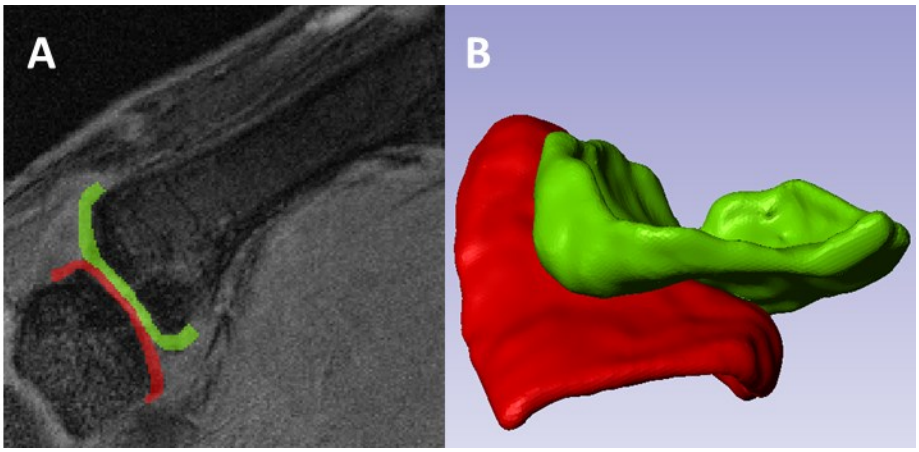


Figure 2.3. (A) Cartilage segmentation from the unloaded image. (B) 3-D cartilage volume generated in ScanIP.

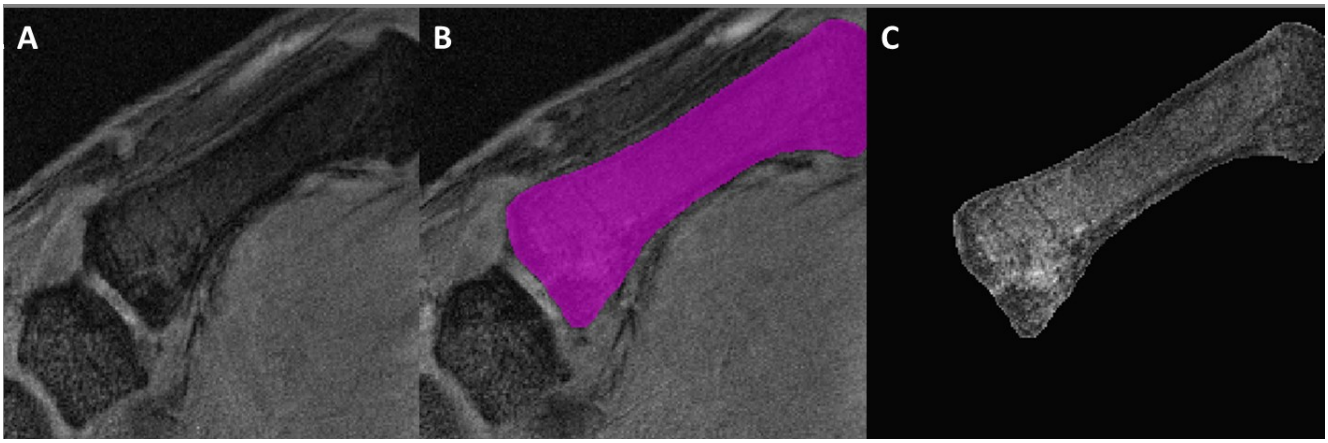


Figure 2.4. Unloaded image without mask (A), the segmented (B) and isolated (C) metacarpal bone without cartilage.

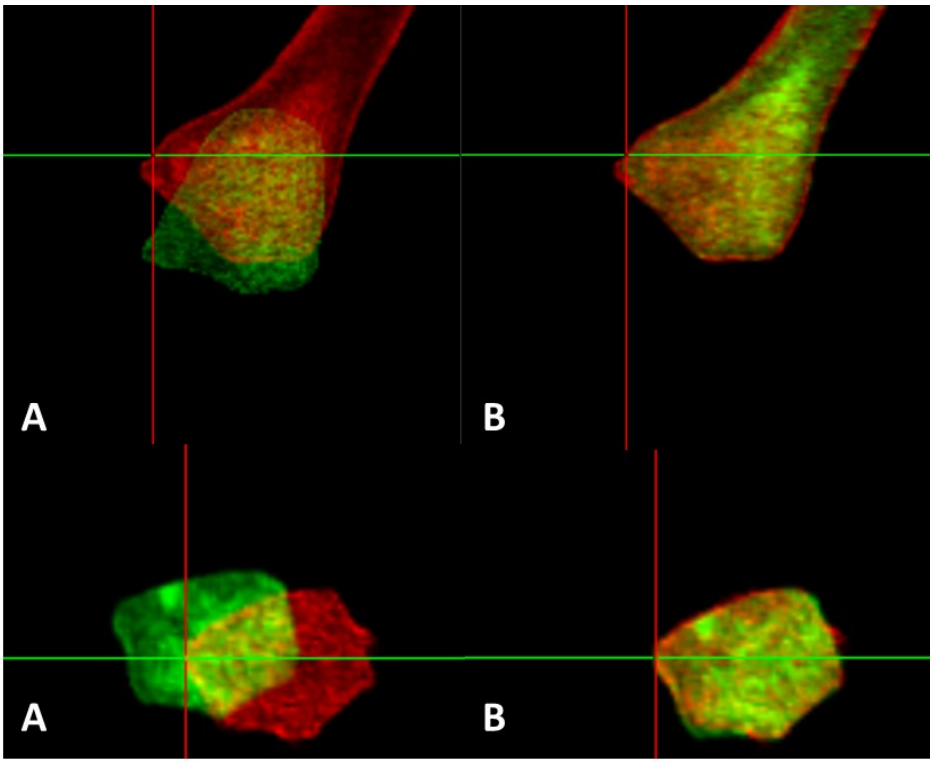


Figure 2.5. Top: registration of loaded metacarpal (green) onto unloaded metacarpal (red). Bottom: registration of unloaded trapezium (green) onto transformed-loaded trapezium (red). Initial position is left (A), and aligned position is right (B).

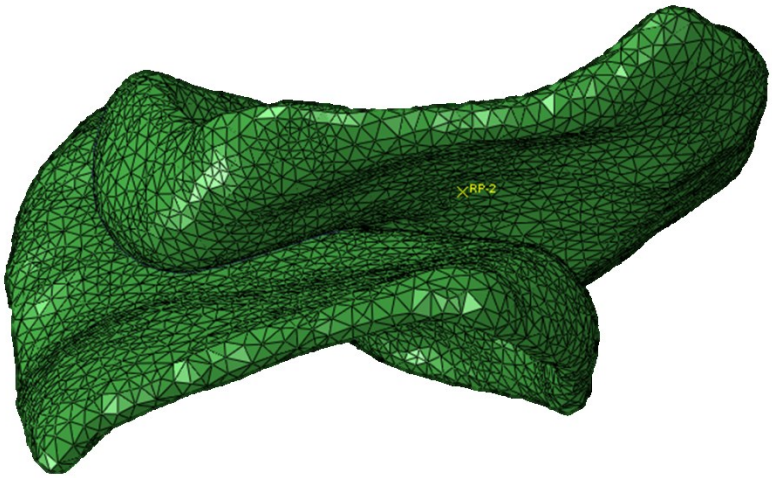


Figure 2.6. Final finite element meshes of the trapezium cartilage (bottom) and metacarpal cartilage (top) articulation in the unloaded configuration in Abaqus. RP-2: reference point for the rigid body constraint.

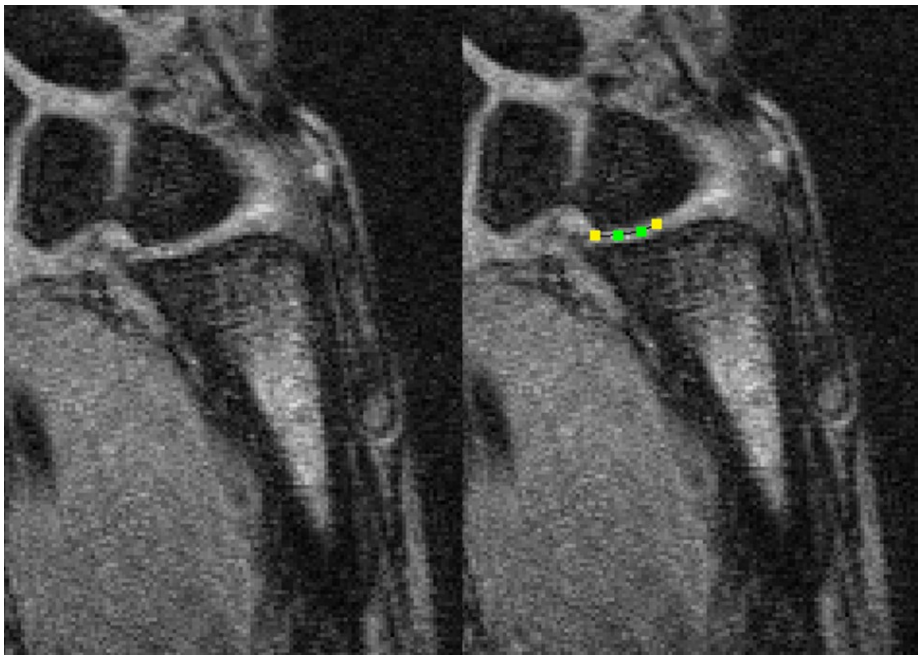

Figure 2.7. Example segmentation of direct contact area determined from a loaded image.

Figure 2.8. MRI image of Subject F4 with osteophyte marked by the red circle.

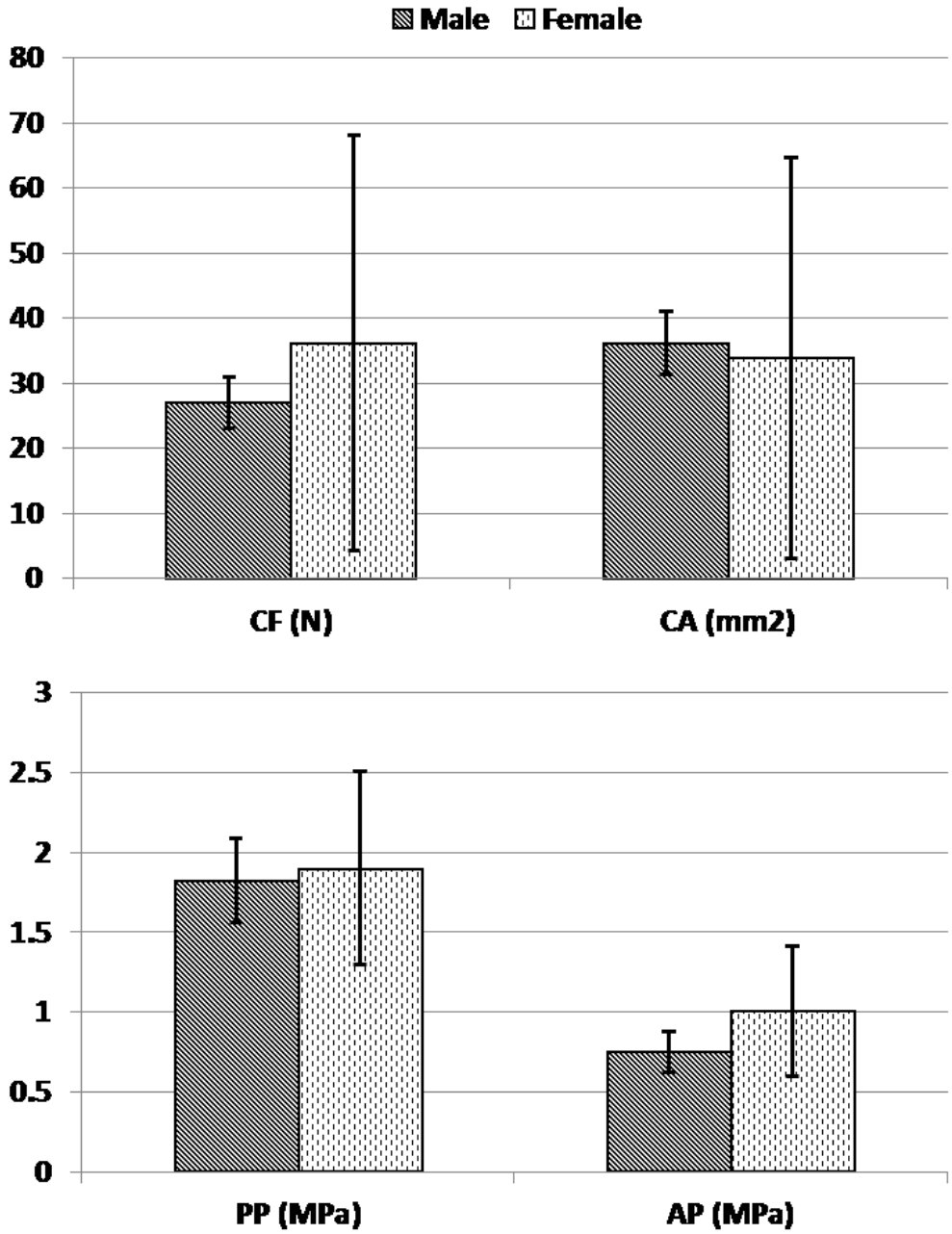


Figure 2.9. Mean value and standard deviation of contact measures for male and female groups.

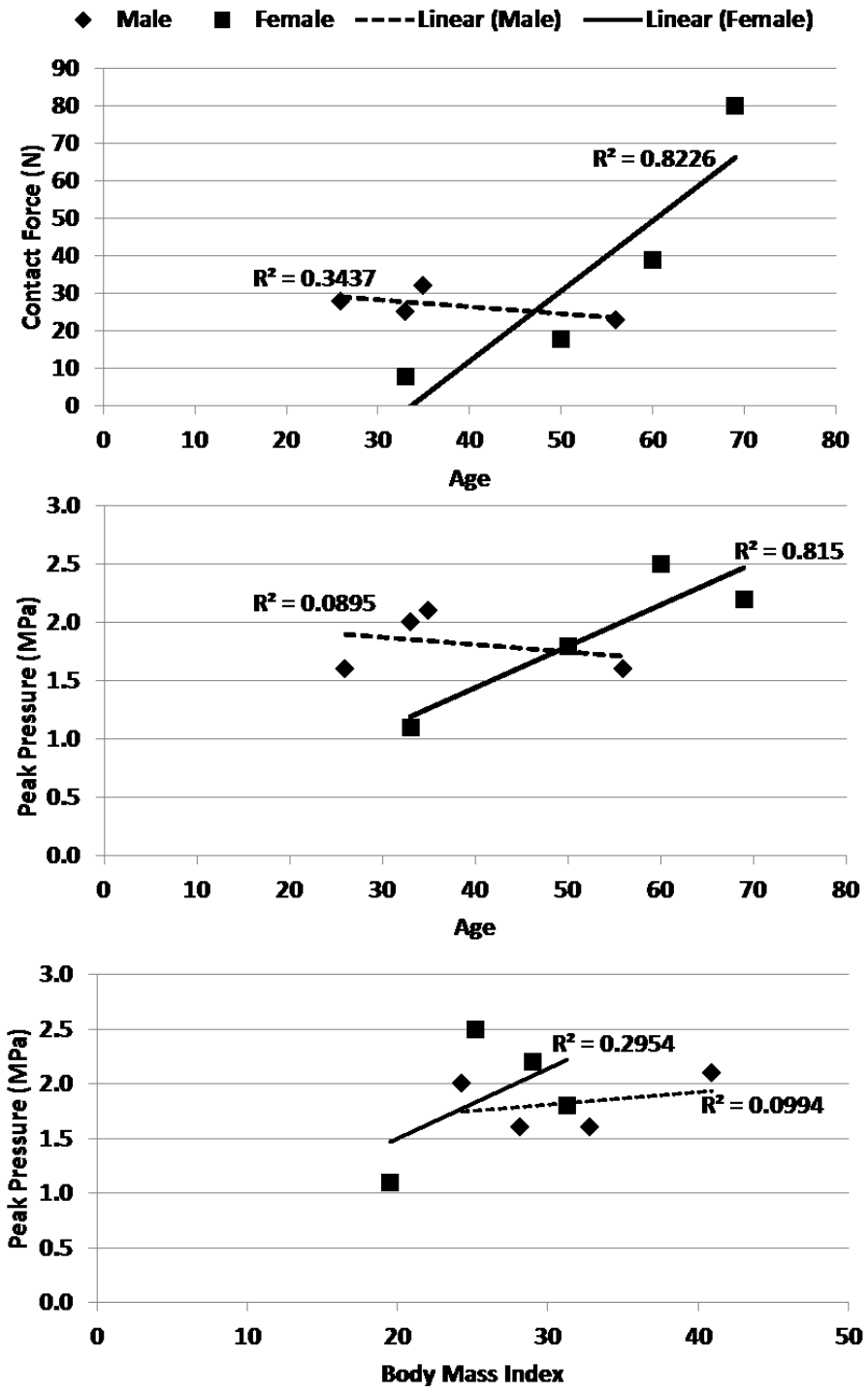


Figure 2.10. Regression of contact force onto age (top), peak pressure onto age (middle), and peak pressure on to body mass index (bottom) for males and females.

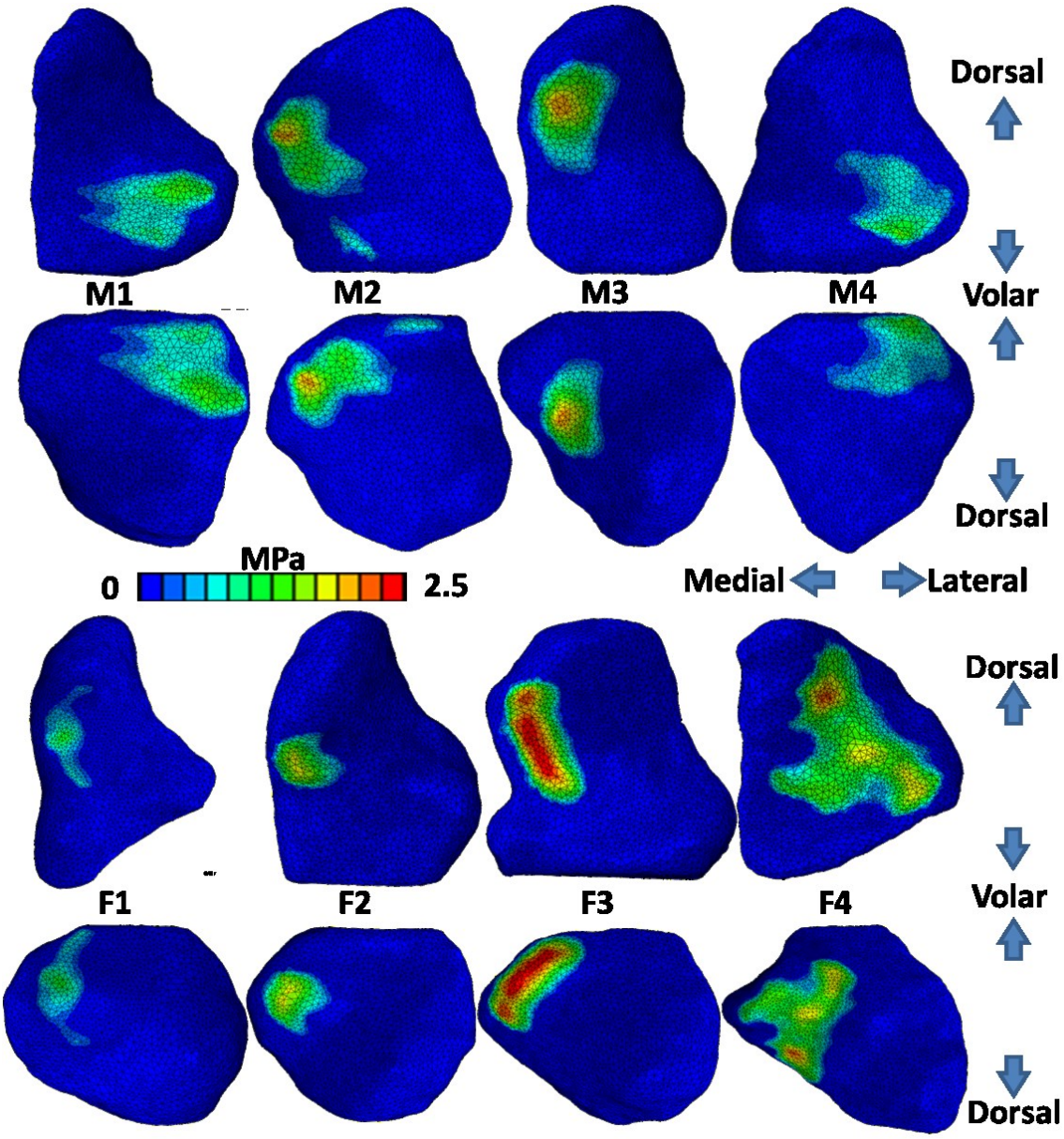


Figure 2.11. Contact distribution on the trapezium and metacarpal for all subjects. Row 1: male trapezium; Row 2: male metacarpal; Row 3: female trapezium; Row 4: female metacarpal.

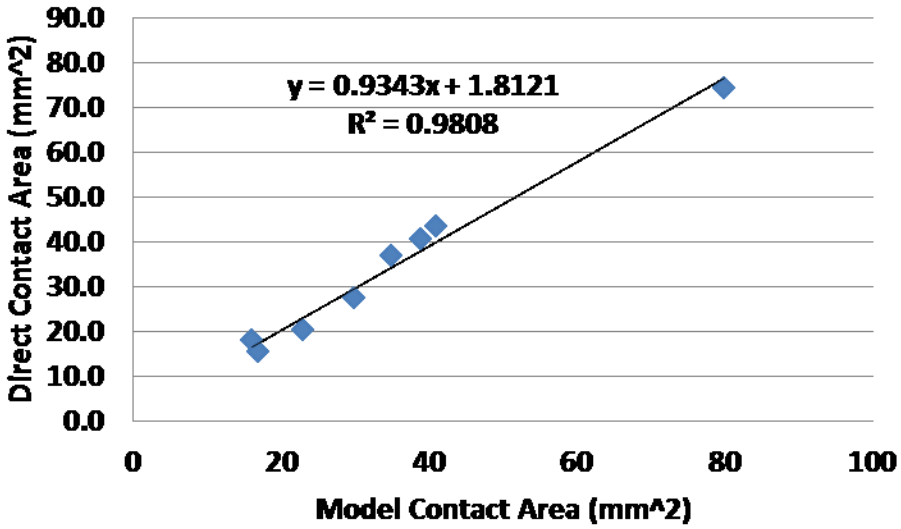


Figure 2.12. Regression analysis of direct contact area and model contact area for all subjects, indicating a highly linear, significant relationship.

This page left intentionally blank.

# 3 *In Vivo* Thumb Carpometacarpal Joint Contact Mechanics: Comparison of Finite Element Modeling and Surface-based Contact Modeling

This page left intentionally blank.

Formatted for submission to Computer Methods in Biomechanics and Biomedical Engineering

# *In Vivo* Thumb Carpometacarpal Joint Contact Mechanics: Comparison of Finite Element Modeling and Surface-based Contact Modeling

Q.Zheng[a], P.Lee[b], T.E.McIff[c], E.B.Toby[c], K.J.Fischer[a, c, d]

[a]*Department of Bioengineering, University of Kansas, Lawrence, USA*

[b]*Hoglund Brain Imaging Center, University of Kansas Medical Center, Kansas City, USA*

[c]*Department of Orthopedic Surgery, University of Kansas Medical Center, Kansas City, USA*

[d]*Department of Mechanical Engineering, University of Kansas, Lawrence, USA*

Kenneth J. Fischer[a,b,*]

1530 W. 15th St. 3138 Learned Hall, Lawrence, KS 66045, USA

Tel: +1 785 864 2994; Fax: +1 785 864 5254

fischer@ku.edu

This page left intentionally blank.

## 3.1 Abstract

Understanding thumb carpometacarpal (CMC) joint contact mechanics is important for early detection of and intervention for thumb CMC osteoarthritis (OA). Based on Magnetic Resonance Imaging (MRI) during functional loading from three asymptomatic female subjects, a time-efficient surface-based contact modeling (SCM) procedure was evaluated for its accuracy compared to finite element modelling (FEM) in predicting in vivo thumb CMC joint contact data. The results suggested that the contact pressure value from SCM is somewhat lower than from FEM. However, SCM predicts contact distribution patterns consistent with FEM, and therefore may have potential for clinical risk assessment, diagnosis and evaluation of thumb CMC OA.
Keywords: thumb carpometacarpal osteoarthritis; joint contact mechanics; finite element modeling; surface-based contact modeling.

## 3.2 Introduction

Thumb carpometacarpal (CMC) osteoarthritis (OA) affects 1 in 12 men and 1 in 4 women (Shuler et al. 2008). The prevalence predominates in postmenopausal women with more than 50% of them complaining of pain at the thumb base (Armstrong et al. 1994). While it is believed that thumb CMC OA is related to both mechanical factors (ligament laxity, dynamic stability, articular surface congruency, etc.) and biochemical factors (hormones and local inflammatory response), so far the etiology of thumb CMC OA remains unclear.

Although radiography has long been used for the staging of thumb CMC OA, it has a very poor correlation with symptoms such as pain and weakness (Barron et al. 2000), which greatly hinders the development of early diagnosis and intervention techniques for thumb CMC OA. Often times,

a patient with a greatly deteriorated thumb CMC joint will not have notable symptoms and therefore will not seek medical assistance. By the time the thumb CMC OA is detected, it has already progressed to the end stages. Trapeziectomy is the primary surgical procedure to achieve pain relief for end-stage thumb CMC OA. The procedure requires a long recovery period and results in shortened thumb length, reduced strength, and reduced hand working space. Though pain is reduced, the outcome still negatively affects the patients' quality of life and may lead to further joint degeneration such as the scaphoid-trapezium OA (Barron, et al. 2000, Martou et al. 2004, Pomerance 1995). Understanding the mechanism of thumb CMC OA development may provide important guidance for developing prevention, early diagnosis, and treatment techniques. Previous studies have indicated that joint contact can be an important factor to evaluate joint stability and OA risk/development (Andriacchi et al. 2004, Ateshian et al. 1992). The contact pressure distribution on the articular surface directly affects the regulation and maintenance of cartilage integrity throughout the lifetime (Andriacchi, et al. 2004). Concentrated stress is more likely to damage the collagen and proteoglycan matrix and cause cartilage degeneration (Ateshian, et al. 1992, Shi et al. 1995). Several studies of thumb CMC joint contact mechanics have been conducted based on the cadaveric models, but the findings are inconsistent (Momose et al. 1999, Ateshian et al. 1995, Pellegrini et al. 1993). At this time we have not found any published data on the *in vivo* thumb CMC joint contact mechanics in normal or pathologic joints. Computational modeling can be an effective and non-invasive tool to measure *in vivo* joint contact mechanics and to evaluate the changes due to gender, age and OA development. Finite element modeling (FEM) and surface-based contact modeling (SCM) are two possible computational methods. FEM is typically considered most accurate and accepted as a gold

standard, but FEM requires substantial manual input to assure a quality mesh, as well as longer computation times. SCM simplifies the model construction and computations, since only the surface-based interaction is considered (Kwak et al. 2000). Thus SCM greatly reduces the analysis time. However, SCM is based on a lower order estimation and may be less accurate. The objective of the current study is to obtain preliminary *in vivo* thumb CMC contact pressure data and to evaluate the accuracy of SCM compared to FEM in order to determine SCM analysis accuracy for possible future research and clinical applications.

## 3.3 Methods

### 3.3.1 Subjects and MRI Scan

Three female subjects with no reported thumb CMC OA symptoms or previous injury to the thumb CMC joint were enrolled for this study (approved by governing IRB). For each subject, one hand was scanned in a 3T clinical MRI system (Siemens Skyra, Siemens, USA) with dual echo steady state (DESS) sequence. Two sets of MRI images were acquired for each hand. First, a high resolution (0.22 mm × 0.2 mm in-plane pixel size, 0.5 mm slice thickness) unloaded image set was acquired with the relaxed hand placed in a flat palm down position (Figure 3.1, top). Then, the same hand performed a functional light grasp by gripping an air-pressurized tube (initial pressure = 3.0 psi = 20.7 kPa) to the target pressure (3.125 psi = 21.5 kPa). The loaded image set was acquired at a relatively lower resolution (0.31 mm × 0.31 mm in-plane pixel size, 1.0 mm slice thickness) in order to reduce the scan time and minimize the subject fatigue and motion artifacts during grasp. All the subjects were required to wear a wrist brace while performing the grasp to ensure consistent wrist position during grasp (Figure 3.1, bottom). The

real-time tube pressure was projected to a computer screen visible to the subjects in the MRI scanner in order to give feedback to the subjects and allow them to maintain the target grasp pressure.

### 3.3.2 Model Geometry Construction

The model geometry of both FEM and SCM were constructed from the unloaded image set. For the SCM analysis, the trapezium and metacarpal bones with cartilage were segmented using ScanIP (Simpleware Ltd, Exeter, UK) (Figure 3.2, top), then the STL surface file was converted to a bilinear 3d surface file using a Matlab surface fitting algorithm. The average surface element edge length was between 0.3 - 0.5 mm for metacarpal and 0.3 - 0.4 mm for trapezium (Table 3.1, Figure 3.3).

In order to evaluate the effect of cartilage thickness on SCM model accuracy, the corresponding subchondral bone surface was also converted to a bilinear 3d surface. For each node from the cartilage surface, a corresponding node from the subchondral bone surface was obtained with the shortest distance from this cartilage surface node to determine the local cartilage thickness. Therefore a spatially varying cartilage thickness file was created specifically for each articular surface for all three thumb CMC joints. The average cartilage thickness of each articular surface (mean of all the values in each thickness file) was calculated (Table 3.1).

For the FEM analysis, the trapezium and metacarpal cartilage only were segmented (with the same articular and subchondral surfaces as in SCM) to create 3-D linear tetrahedral volume mesh using the ScanIP/FE module (Figure 3.2, bottom). Two sequential mesh refinements were performed for each thumb CMC joint in order to assure mesh convergence. For each modeling analysis, less than 5% variation of contact force was used as the mesh convergence criterion. The

FEM mesh convergence criterion was achieved by increasing the number of nodes from 3515 to 8600 for the metacarpals and from 4198 to 6015 for the trapeziums. After refinement, the average element side length was between 0.3 – 0.7 mm for both metacarpal and trapezium cartilage (Table 3.1, Figure 3.3). For each joint, the converged mesh was also converted to quadratic tetrahedral elements and the same contact parameters were computed.

### 3.3.3 Kinematics

The kinematic transformations for the bones to the state of light grasp were obtained using image registration of the trapezium and metacarpal from the unloaded to the loaded configuration, based on the assumption that the deformation of the bones during light grasp loading was negligible. The trapezium and metacarpal bones without cartilage were segmented and isolated from the unloaded and loaded image sets. The registration was performed using Analyze 5.0 voxel-based registration module, because voxel registration is less sensitive to segmentation errors. The metacarpal was used as the reference in the unloaded and loaded coordinate systems. First the loaded metacarpal was registered to the unloaded metacarpal to obtain the transformation that aligned the loaded image set with the unloaded coordinate system (Figure 3.4 top). Then the loaded trapezium was transformed into the unloaded coordinate system using this loaded-to-unloaded reference transformation. Finally the unloaded trapezium was registered to the transformed-loaded trapezium in order to obtain the kinematic transformation from the unloaded to the loaded configuration (Figure 3.4, bottom).

### 3.3.4 Modeling Analyses and Verification

For each thumb CMC joint, the contact mechanics were analyzed using FEM with linear tetrahedral mesh (FEML), FEM with quadratic tetrahedral mesh (FEMQ), SCM with uniform

cartilage thickness (SCMU), and SCM with variable cartilage thickness (SCMV). All four procedures were performed with displacement boundary conditions. For each analysis, the obtained kinematic transformation was applied to the trapezium while the metacarpal was fixed. Within each subject, the contact area (CA), contact force (CF) and peak contact pressure (PP) were compared among the four different methods.

The SCM was performed using Joint_Model for the Windows operating system. For the SCMU analysis, the cartilage thickness was assumed to be 1 mm; for the SCMV analysis, the subject-specific cartilage thickness file was incorporated for each model. The rigid surface linear contact rule was applied in SCM, hence the local contact pressure was proportional to the local strain and the local strain was calculated as the local surface interpenetration divided by the total local cartilage thickness. The effective cartilage relaxation modulus, for all subjects and bones, was set to 4 MPa (Kwak, et al. 2000, Johnson et al. 2012, Fischer et al. 2011). The contact area was determined by the overlapping region of the two articular surfaces. The contact force was calculated as the local contact pressure integrated over the entire contact area.

The FEM was performed using Abaqus 6.9 (Simulia, Providence, RI). The cartilage was modeled as an elastic solid with homogeneous and isotropic material properties. The cartilage Young's modulus was modeled as 4 MPa (effective relaxation modulus) and Poisson's ratio = 0.2 (Jurvelin et al. 1997). Frictionless contact with finite sliding was assumed for the cartilage articulation.

In order to verify the accuracy of the modeling procedures, for each thumb CMC joint the contact area was also directly measured from the loaded MRI and compared with the contact area calculated from the modeling analysis. The contact region curve was segmented from each

loaded image slice. The lengths of image contact curves were calculated, multiplied by the slice thickness and summed to obtain the total contact area (Figure 3.5).

## 3.4 Results

Although all three subjects self-reported asymptomatic, Subject 3 showed substantial joint space narrowing, cartilage degeneration and osteophyte formation, which strongly indicated an advanced stage of thumb CMC OA (Figure 3.6). The average cartilage thickness for Subject 3 was also lower than that of Subject 1 and 2 for both articular surfaces (Table 3.1).

The pressure distribution maps showed that Subject 1 and 2 had similar contact patterns, with primary contact located at the center of the medial edge, while Subject 3 showed much larger contact area with the PP location shifted substantially in the dorsal direction compared with the first two subjects. Within each subject, the pressure distribution from FEM and SCM analyses were very similar (Figure 3.7), though the PP values varied between FEM and SCM (Figure 3.8). For the two FEM analyses, the pressure distribution inside the cartilage and on the subchondral surface showed similar patterns with the articular surface contact pressure, while the pressure values were sometimes higher inside the cartilage, compared to the articular surface, especially near the rigid back-side boundary condition (Figure 3.9).

For all three subjects, the computed contact parameters from FEML and FEMQ were very similar (Figure 3.8, Figure 3.10, Table 3.2). The PPs from the two FEM analyses were higher than that from the two SCM analyses. Comparing the two SCM analyses, the PP from SCMV was higher than that from SCMU for Subject 2 and 3 while similar for Subject 1 (Figure 3.8). The FEM results in particular appeared to indicate that Subject 3, with OA symptoms, had

somewhat higher PP. For Subject 1, CF from the two SCM procedures was similar and higher than FEM. For Subject 2 and 3, CF from FEM was higher than that from SCMU and SCMV, though SCMV yielded CF closer to FEM (Figure 3.10).

Regarding the time efficiency, time to build a single finite element model and prepare an adequate mesh (including convergence studies) was approximately 6 hours compared to 30 minutes for the SCM surface mesh. In addition, FEML computation took 20 minutes and FEMQ took about 1 hour, compared to 3 seconds for the two SCM procedures (all comparisons made using a Windows PC with 12 processors (3.30 GHz), and 64 Gb of RAM).

The subject-specific measure of model fidelity is the comparison with direct contact area. The direct contact areas measured from the loaded images were within 15% variation from FEM computed CAs, which indicated the level of accuracy for FEM modeling procedures. CAs computed from SCM were consistently larger than FEM and direct contact area (Table 3.2).

## 3.5 Discussion

In this study, Subject 3, although self-reported asymptomatic, showed clear radiographic evidence of thumb CMC OA and substantially altered joint contact pattern compared with the other two subjects. This aligns with the previous findings that the radiographic evidence of thumb CMC OA correlates poorly with the symptoms, and is also consistent with the prior cadaveric studies suggesting substantial changes in joint contact with OA development (Momose, et al. 1999, Ateshian, et al. 1995, Pellegrini, et al. 1993). For a clinical application of SCM to evaluate the *in vivo* joint contact mechanics, the goal is to detect adverse joint mechanics before radiographic or MRI evidence of thumb CMC OA.

Both FEM and SCM are computational modeling procedures that have been used for analyzing *in vivo* joint contact mechanics. However, we have found no published study applying either procedure to *in vivo* thumb CMC joint contact mechanics. FEM applies deformable analysis, which typically yields more accurate results by accounting for deformation within the entire cartilage volume. In the current study, FEM consistently had higher PP than both SCM analyses for all three subjects. The higher PP for FEM may be partially due to the different meshes and element types used in FEM and SCM. Although the average element edge length showed no substantial difference between these two methods, the SCM mesh was very uniform and FEM included many smaller elements. Thus, locally smaller elements in FEM may have better approximated the true PP (Table 3.1, Figure 3.3). Although *linear* tetrahedral elements are believed to have stiffer response and cause overestimation of PP, no apparent differences between FEML and FEMQ were observed, which suggests that the stiffening of *linear* tetrahedral elements was negligible in theses analyses.

Our FEM analysis incorporated several simplifications including the use of linear tetrahedral element and the rigid subchondral bone constraint, which could also lead to overestimation of PP. Even with those simplifications, the FEM still took much longer time than SCM. The long preparation and computation time for FEM is a drawback that may limit the application of FEM in clinical practice, where rapid processing is required.

Previous studies have suggested that elevated and/or concentrated contact pressure exerted on the articular surface is more likely to damage the cartilage collagen and proteoglycan matrix and therefore induce OA development (Ateshian, et al. 1992, Shi, et al. 1995). Thus PP is a key measure for predicting OA risk. Because the SCM analysis used in this study was based on a

linear surface interaction contact rule, the contact pressure values were expected to be somewhat less accurate than FEM. While SCM PP was quantitatively lower than FEM PP, SCM produced the same trends for PP across the subjects, and very similar contact distributions (i.e. changes of CA and PP location). PP location is also a key measure, since it indicates shifts in loading that may induce OA. Thus, SCM may be capable of providing sufficient information for future clinical applications with much less modeling time.

CAs from SCM were consistently higher than FEM and direct contact area. This is most likely due to the rigid body surface interaction assumption in SCM. FEM had similar pressure distribution patterns inside the cartilage as with that on the articular surface, which may suggest that surface contact analysis may be sufficient to provide information about the stress exerted on the cartilage. The higher pressure values inside cartilage and on the subchondral may be due to the rigid subchondral surface assumption. However, further study is needed to confirm the cause of such pattern, as well as to determine whether such elevated the pressure values will have significant effects on cartilage conditions.

In the current study we also investigated the effect of incorporating cartilage thickness on the SCM joint contact analysis accuracy, as the contact pressure and pressure distribution on the articular surface is clearly directly related to cartilage thickness which may be altered due to degeneration (Andriacchi, et al. 2004, Ateshian, et al. 1992, Shi, et al. 1995). Thinner cartilage will increase the local strain and contact pressure. Incorporating the cartilage thickness file was shown to improve the SCM model accuracy (calculation of CF and PP) compared to FEM for both Subjects 2 and 3.

This study had several limitations. Because of the small number of subjects, there is no reasonable basis for statistical comparisons of the obtained data. Also, FEM was performed using linear tetrahedral elements, which can lead to stiffening of the model response (for a given modulus) compared to higher order elements. For the future studies, FEM analysis should be evaluated using quadrilateral tetrahedral elements or hexahedral elements to prevent this stiffening response. Also the rigid body constraint for subchondral cartilage surface may have increased the effective cartilage stiffness and yielded higher PP results, which may be part of the reason that PPs from FEM were higher than PPs from SCM in all three subjects. Thus, modeling and moving the deformable bones with cartilage should be considered in future FEM studies. However, this will further increase the model and mesh preparation time as well as the computation time.

In the current study, the actual cartilage modulus is unknown and cannot be determined in a non-invasive manner. In addition, cartilage material properties are likely to change in the degenerated thumb CMC joint. Therefore for Subject 3 the 4 MPa Young's modulus and 0.2 Poisson's ratio may not be accurate. These material properties will directly affect the PP calculation for both FEM and SCM analyses. One study clearly indicated that joint degeneration and OA development will cause decreased cartilage modulus (Boschetti and Peretti 2008). Using the same modulus for Subject 3, with evidence of OA, may have contributed to the higher PP. That is, if a lower modulus had been used to account for OA degeneration, then Subject 3 PP may have been similar or even lower than the PP of the other subjects.

## 3.6 Conclusion

This study compared surface-based contact modeling and finite element modeling for *in vivo* thumb CMC joint contact mechanics analysis. The results suggested that SCM can provide relative contact mechanics measures similar to those from FEM, and SCM is able to model both normal and osteoarthritic subjects. In addition, using variable cartilage thickness in SCM improves the prediction accuracy, as expected. Therefore, SCM has clear potential for future research and clinical applications exploring the etiology of thumb CMC OA, including risk assessment, prevention, diagnosis, and treatment options based on *in vivo* joint contact mechanics.

## 3.7 Acknowledgements

We would like to acknowledge support for the study from the National Institute of Biomedical Imaging and Bioengineering of the National Institutes of Health under award R01EB008709, and technical assistance from Allan Schmitt and Frank Hunsinger, We thank Gerard Ateshian and Columbia University as well as Leendert Blankevoort and the Academic Medical Center of Armsterdam for providing Joint_Model software and support.

## 3.8 Reference

Shuler MS, Luria S, Trumble TE. 2008. Basal joint arthritis of the thumb. The Journal of the American Academy of Orthopaedic Surgeons. 16(7):418-423.

Armstrong AL, Hunter JB, Davis TR. 1994. The prevalence of degenerative arthritis of the base of the thumb in post-menopausal women. J Hand Surg Br. 19(3):340-341.

Barron OA, Glickel SZ, Eaton RG. 2000. Basal joint arthritis of the thumb. The Journal of the American Academy of Orthopaedic Surgeons. 8(5):314-323.

Martou G, Veltri K, Thoma A. 2004. Surgical treatment of osteoarthritis of the carpometacarpal joint of the thumb: a systematic review. Plast Reconstr Surg. 114(2):421-432.

Pomerance JF. 1995. Painful basal joint arthritis of the thumb. Part II: Treatment. Am J Orthop (Belle Mead NJ). 24(6):466-472.

Andriacchi TP, Mundermann A, Smith RL, Alexander EJ, Dyrby CO, Koo S. 2004. A framework for the in vivo pathomechanics of osteoarthritis at the knee. Ann Biomed Eng. 32(3):447-457.

Ateshian GA, Rosenwasser MP, Mow VC. 1992. Curvature characteristics and congruence of the thumb carpometacarpal joint: differences between female and male joints. J Biomech. 25(6):591-607.

Shi Q, Hashizume H, Inoue H, Miyake T, Nagayama N. 1995. Finite element analysis of pathogenesis of osteoarthritis in the first carpometacarpal joint. Acta medica Okayama. 49(1):43-51.

Momose T, Nakatsuchi Y, Saitoh S. 1999. Contact area of the trapeziometacarpal joint. The Journal of hand surgery. 24(3):491-495.

Ateshian GA, Ark JW, Rosenwasser MP, Pawluk RJ, Soslowsky LJ, Mow VC. 1995. Contact areas in the thumb carpometacarpal joint. Journal of orthopaedic research : official publication of the Orthopaedic Research Society. 13(3):450-458.

Pellegrini VD, Jr., Olcott CW, Hollenberg G. 1993. Contact patterns in the trapeziometacarpal joint: the role of the palmar beak ligament. The Journal of hand surgery. 18(2):238-244.

Kwak SD, Blankevoort L, Ateshian GA. 2000. A Mathematical Formulation for 3D Quasi-Static Multibody Models of Diarthrodial Joints. Comput Methods Biomech Biomed Engin. 3(1):41-64.

Johnson JE, McIff TE, Lee P, Toby EB, Fischer KJ. 2012. Validation of radiocarpal joint contact models based on images from a clinical MRI scanner. Comput Methods Biomech Biomed Engin.

Fischer KJ, Johnson JE, Waller AJ, McIff TE, Toby EB, Bilgen M. 2011. MRI-based modeling for radiocarpal joint mechanics: validation criteria and results for four specimen-specific models. Journal of biomechanical engineering. 133(10):101004.

Jurvelin JS, Buschmann MD, Hunziker EB. 1997. Optical and mechanical determination of Poisson's ratio of adult bovine humeral articular cartilage. J Biomech. 30(3):235-241.

Boschetti F, Peretti GM. 2008. Tensile and compressive properties of healthy and osteoarthritic human articular cartilage. Biorheology. 45(3-4):337-344.

## 3.9 Tables and Figures

Table 3.1. Element edge length (mm) data from FEM and SCM, and cartilage thickness (mm) of metacarpal and trapezium for all subjects.

| | Metacarpal | | | | Trapezium | | | |
|---|---|---|---|---|---|---|---|---|
| | FEM Average Min | FEM Average Max | SCM Average | Cartilage Thickness | FEM Average Min | FEM Average Max | SCM Average | Cartilage Thickness |
| Subject 1 | 0.37 | 0.69 | 0.33 | 0.90 | 0.34 | 0.60 | 0.33 | 0.82 |
| Subject 2 | 0.37 | 0.70 | 0.36 | 0.96 | 0.34 | 0.64 | 0.30 | 0.83 |
| Subject 3 | 0.33 | 0.62 | 0.47 | 0.66 | 0.34 | 0.65 | 0.38 | 0.64 |
| Average | 0.35 | 0.67 | 0.39 | - | 0.34 | 0.63 | 0.34 | - |

Table 3.2. Contact area ($mm^2$) from SCM, FEM and Direct Contact Area (DCA).

| | SCM | FEML | FEMQ | DCA |
|---|---|---|---|---|
| Subject 1 | 27 | 16 | 16 | 18 |
| Subject 2 | 26 | 17 | 18 | 15 |
| Subject 3 | 92 | 80 | 82 | 74 |

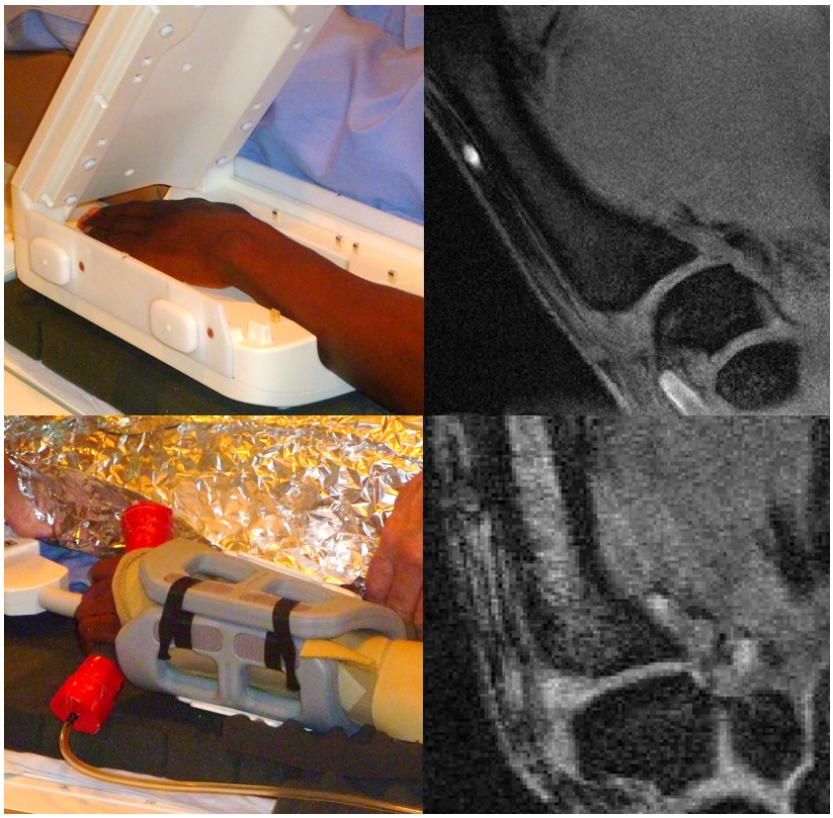

Figure 3.1. Top: Unloaded scan, hand position (left) and MRI image (right). Bottom: Loaded scan, hand position (left) and MRI image (right).

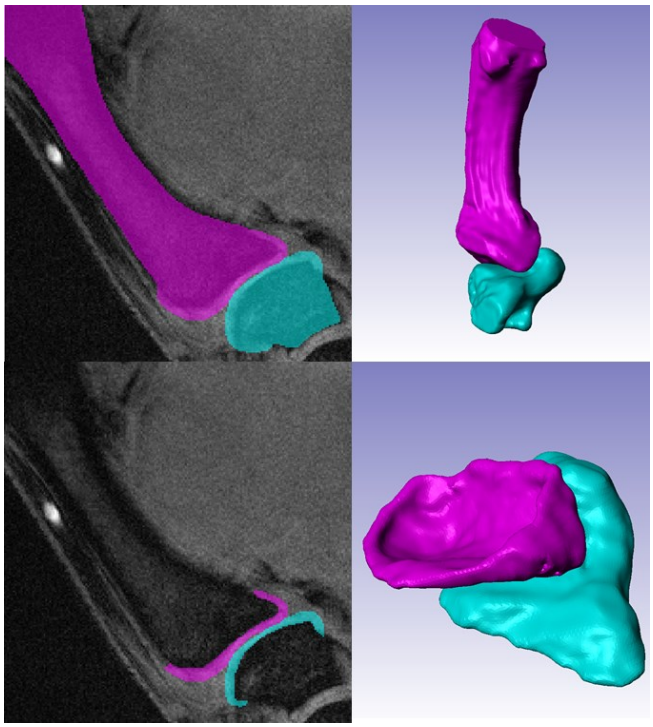

Figure 3.2. Top: Bone with cartilage segmentation (left) and model geometry (right) for SCM. Bottom: Cartilage segmentation (left) and model geometry (right) for FEM.

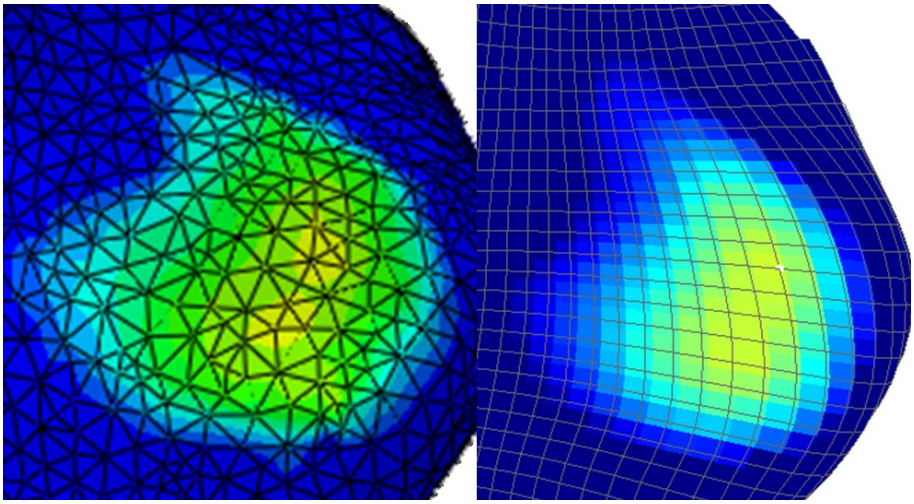

Figure 3.3. Visual comparison of mesh resolution of FEM (left) and SCM (right) in the contact region.

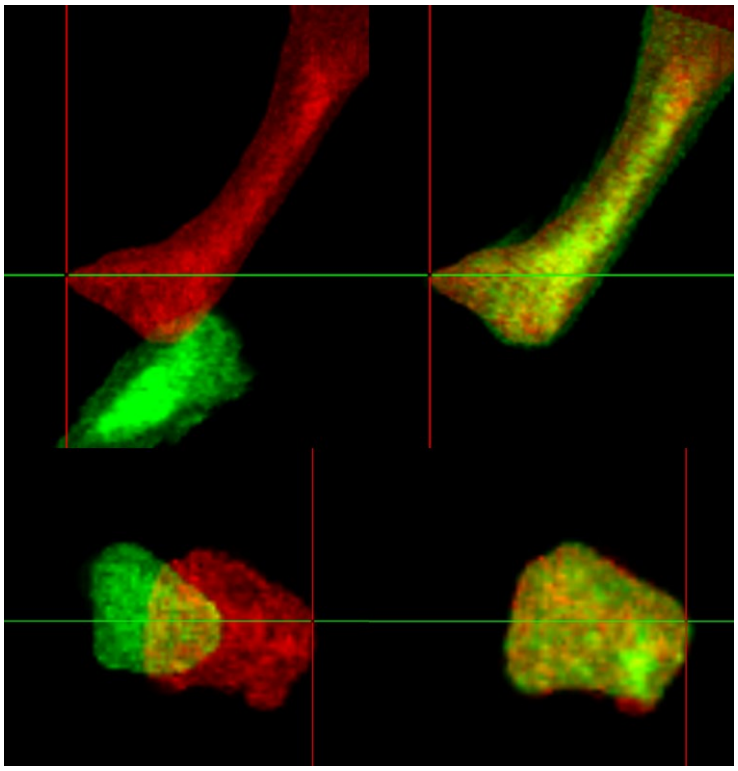

Figure 3.4. Top: loaded metacarpal (green) registered to the unloaded metacarpal (red). Bottom: unloaded trapezium (green) registered to the transformed-loaded trapezium (red). Left: initial position. Right: aligned position.

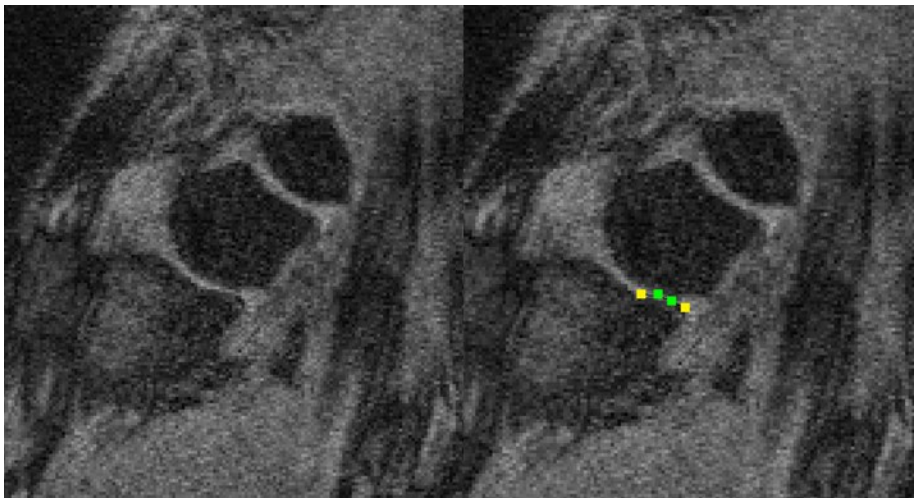

Figure 3.5. Segmentation of contact area directly from the loaded image.

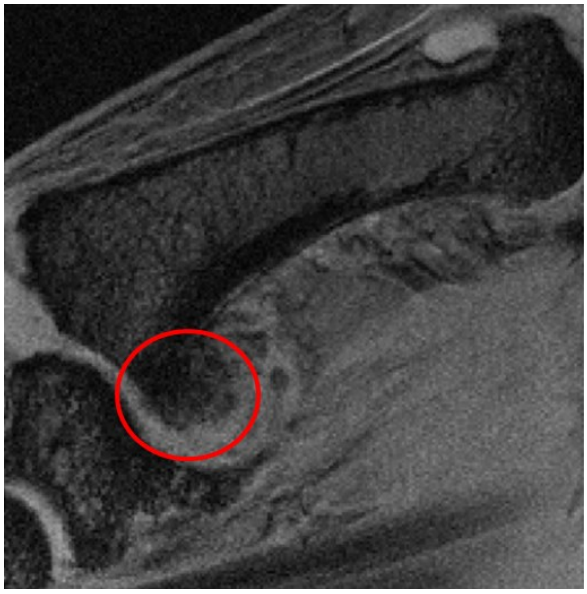

Figure 3.6. MRI image of Subject 3 with osteophyte marked by the red circle.

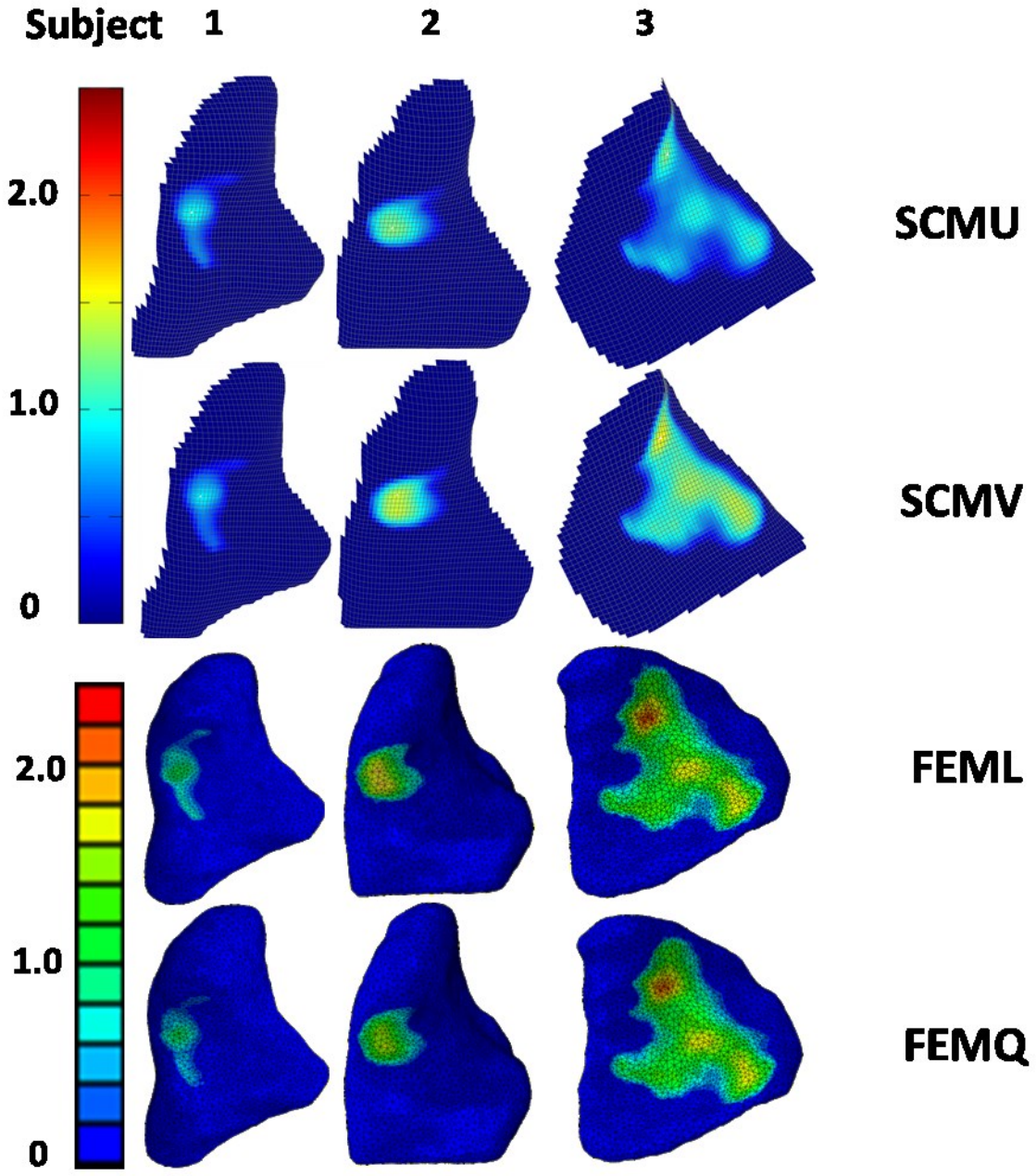


Figure 3.7. Contact pressure distribution on the trapezium cartilage surface.

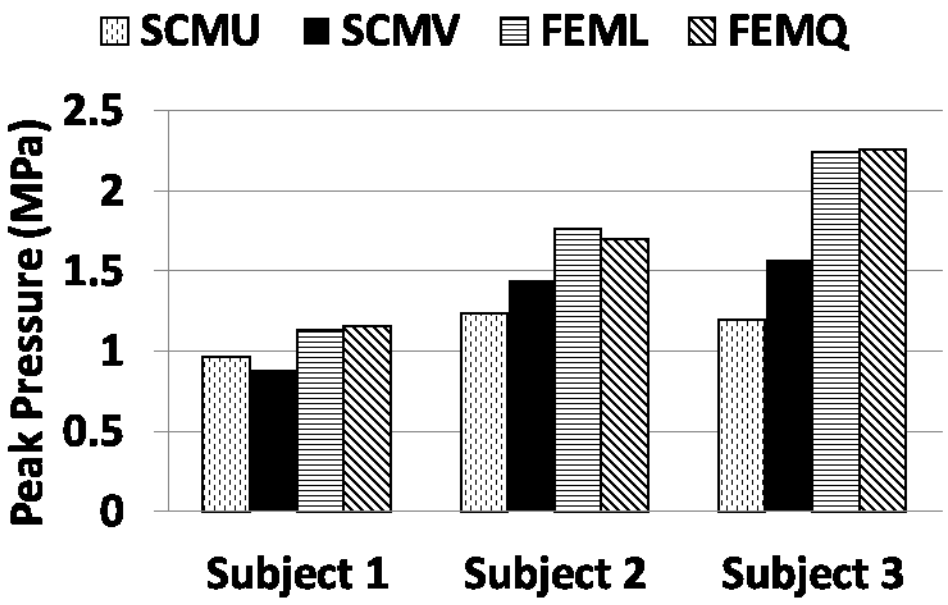


Figure 3.8. Peak pressures computed from SCMU, SCMV, FEML and FEMQ for all three subjects. FEM PPs were consistently higher than SCM PPs.

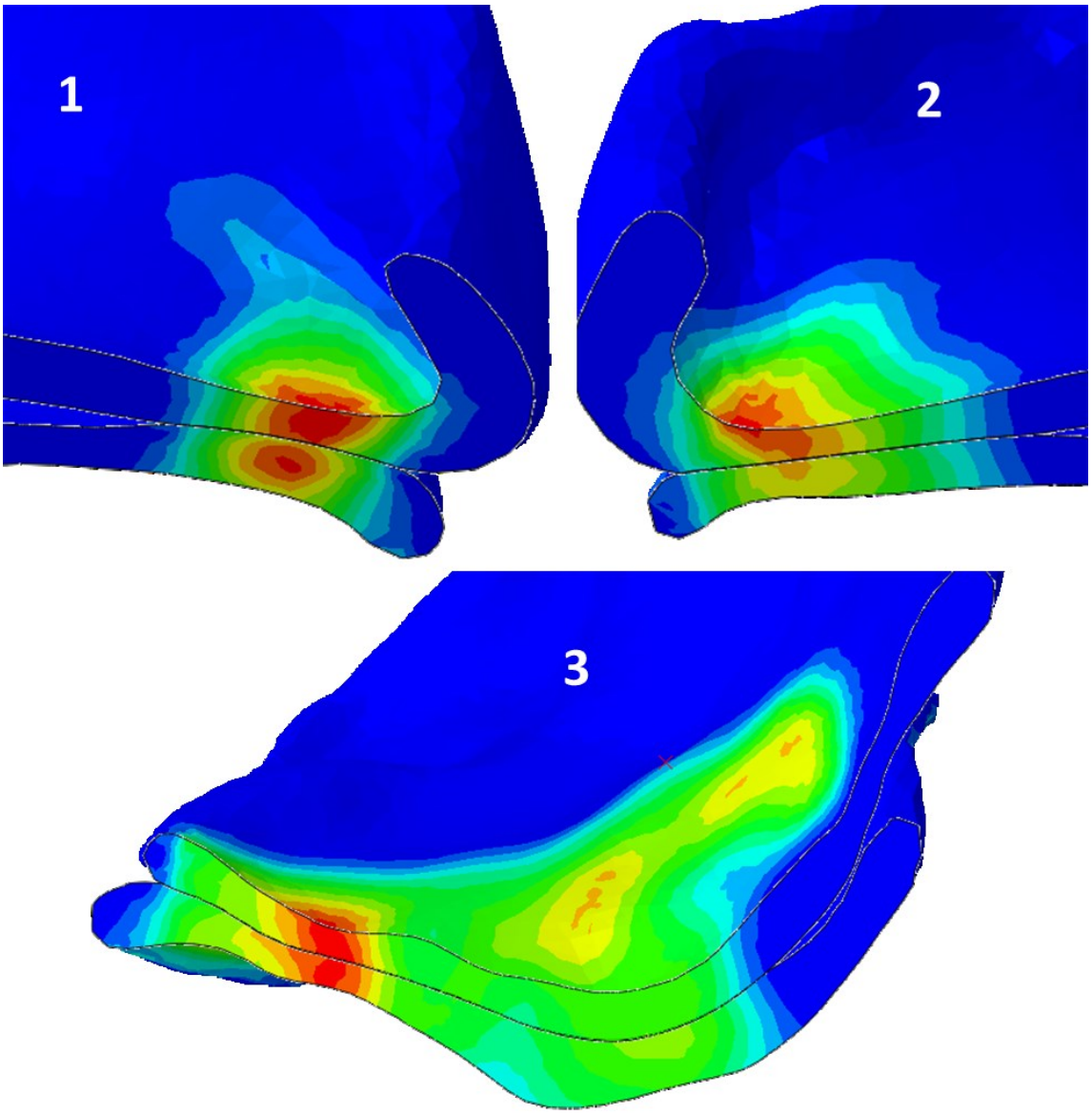


Figure 3.9. Pressure distribution inside the cartilage viewed from a cutting plane for all three subjects. Top: metacarpal cartilage. Bottom: trapezium cartilage.

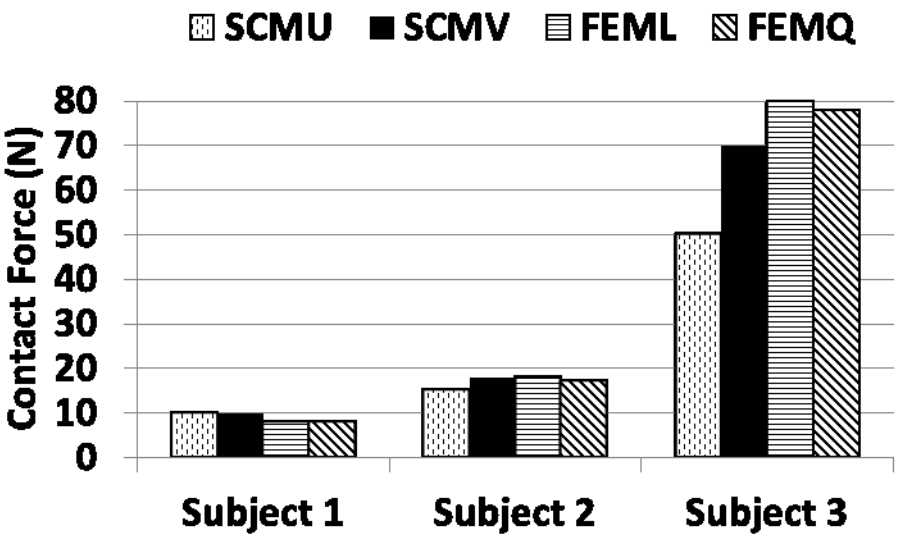


Figure 3.10. Contact forces computed from SCMU, SCMV, FEML and FEMQ for all three subjects.

This page left intentionally blank.

# 4 Conclusion and Future Directions

The comparison of *in vivo* thumb CMC joint contact mechanics between males and females indicated likely differences in primary contact distribution. Although no statistical significance was observed, the linear regression analysis suggested that aging may have more profound effect on contact pressure values of the female thumb CMC joint. As the contact pressure distribution can be directly related to cartilage degeneration, the observed outcomes might indicate the intrinsic incongruent and unstable articulation in female thumb CMC joint, which causes stress distributions that lead to cartilage degeneration over the years. Given the small number of subjects, the above hypothesis has not been proven, and it is confounded by other factors related to the gender differences (e.g. hormonal environment). However, the results from this study show the potential of *in vivo* joint contact mechanics to improve understanding the thumb CMC OA etiology.

For three of the female subjects, the thumb CMC joint contact mechanics data were computed using FEM, SCMU and SCMV. Although the absolute CA and PP values obtained from SCM were quantitatively different from FEM, which is commonly considered the gold standard, SCM can still provide good relative data and accurate contact distribution pattern consistent with FEM. SCM can also detect the alteration of contact pattern due to OA development. Most importantly, the SCM analysis requires much less time, labor input and computational resources. Given the indications from the previous chapter that the *in vivo* contact mechanics can provide insights into thumb CMC OA development, this modeling tool may also be used to develop early diagnosis techniques and/or evaluate the treatment efficacy. While the absolute accuracy of SCM may be a concern, incorporating the cartilage thickness in SCM appears to help increase the computational

accuracy, especially for analyzing degenerated thumb CMC joints, which are more likely to possess abnormal and irregular cartilage thickness.

Findings from these current studies are not completely conclusive, yet they raise the necessity for further investigation and collaboration from engineers, chemists, physicians, etc. For future investigations, the *in vivo* contact mechanics analyses as well as the comparison between FEM and SCM need to be performed on more subjects to achieve conclusions with sufficient statistical power. Meanwhile, when comparing the thumb CMC joint between males and females, other factors such as the hormonal environment causing gender differences also need to be controlled and considered. For example, urine sample can be drawn from each subject to test the estrogen or testosterone level, and the result can be correlated with the contact mechanics data to evaluate possible causal effects or interaction between the mechanical factors and biochemical factors on OA development.

The overall objective of this study is to improve the prevention and early intervention of thumb CMC OA. Therefore another major theme of future study is to develop and evaluate early treatment techniques. For instance, each participant with suspicious abnormal thumb CMC joint contact may undergo simple hand therapy (e.g. exercise to strengthen a specific muscle or muscle group) administered for a certain period of time, and the joint contact mechanics may be re-evaluated after the therapy to assess the efficacy and to provide guidance for improving the therapy protocol.

In conclusion, the *in vivo* thumb CMC joint contact mechanics suggested intrinsic gender differences related to the higher thumb CMC OA risk in postmenopausal women. The time-efficient SCM technique has clear potential for future research and clinical applications.